Extension theory for lattice Green functions

William A. Schwalm and Mizuho K. Schwalm
Department of Physics, University of North Dakota, Grand Forks, North Dakota 58202
(Received 13 November 1987)

A method is presented of using the known Green functions or densities of states (DOS) for a given Hamiltonian H to find Green functions or DOS for any lattice Hamiltonian H_e in the algebra of H, or $H_e=f(H)$. The procedure is further developed to permit using the known Green functions and DOS of two Hamiltonians H and K to obtain those of any Hamiltonian H_e in the algebra generated by the direct products $H\otimes I$ and $I\otimes K$. The method does not depend on translation symmetry, and rather general extension formulas are derived. Several analytical and numerical results are presented as examples. Green functions well known for the nearest-neighbor lattice Hamiltonian in one dimension are used to solve a one-dimensional (1D) second-neighbor model, a 1D model with infinite range, a 2D model on a square lattice with first-, second-, and third-neighbor interactions, a 2D square-lattice model with edges and corners, and a simple-cubic lattice Hamiltonian with surfaces, edges, and corners in three dimensions. Green functions for the threefold-coordinated Sierpiński lattice Hamiltonian treated by O'Shaughnessy and Procaccia are extended to the treatment of a Sierpiński model with first and second neighbors, and then are further extended to treat a new fractal Hamiltonian on the Cartesian product of two Sierpiński lattices. Green functions of the 1D Fibonacci lattice treated by Kohmoto are extended to the treatment of quasiperiodic Fibonacci plaid lattices in two and three dimensions. These lattices are quasiperiodic and admit inflation-deflation transformations, but do not have interesting or forbidden rotation symmetry.

I. INTRODUCTION

The purpose of this paper is to present a means of using the known Green functions of a given lattice Hamiltonian H to find the Green functions of related Hamiltonians.

Here the term lattice is used only abstractly to denote a set of sites spread out in space in a certain way. We assume that on a lattice consisting of a collection of sites, a model for some phenomenon such as spin waves, lattice vibrations, or the behavior of independent electrons, can be defined by a Hamiltonian matrix H. The sites are the index set for H, and for a given lattice there can be many Hamiltonians. The square lattice, for example, can have a Hamiltonian with elements connecting only nearest-neighbor sites, or it can have another Hamiltonian that connects also second-neighbor sites. The lattices treated in the following sections may or may not have translation symmetry.

The Green function $G_{ij}(z)$ is the (i,j) element of the resolvent matrix $G(z)$ defined for each z outside the spectrum of H by

$$G(z)=[zI-H]^{-1} \tag{1}$$

with I the identity on the lattice of H. Green functions for 1D lattice Hamiltonians have been treated by Dyson,[1] and the second-neighbor case has been solved in some detail by Davison and Levine.[2] Green functions for nearest-neighbor interactions on finite chains have been found by Bass[3] for various boundary conditions. Green functions for basic Hamiltonians on 2D and 3D lattices have been computed in terms of complete elliptic integrals by Morita and co-workers.[4–9]

Using the known Green functions of a given Hamiltonian H, or of a pair of Hamiltonians H and K, to compute Green functions for a related Hamiltonian H_e will be referred to as extending the Green functions of H, or of H and K, to the Green functions of H_e. Likewise, we speak of extending the densities of states (DOS).

Two kinds of extensions are presented below. In the first, the Green functions or DOS of H are extended to those of another Hamiltonian H_e on the same lattice. The basic idea is that it is easy to do the extension to a particular set of Hamiltonians having the same eigenvectors as H, namely, the algebra generated by H. An element of the algebra generated by H is of the form

$$H_e=a_0I+a_1H+a_2H^2+\cdots=\sum_n a_nH^n=f(H) \tag{2}$$

where the coefficients are real and the sum is over all independent powers of H. It is assumed for the time being that singularities of $f(x)$ lie outside a circle in the complex plane containing the eigenvalues of H. Not all Hamiltonians on the lattice of H can be expressed in this form, but if H is uncomplicated and physically reasonable, then its algebra contains many other physically reasonable Hamiltonians of a more complicated form. For example, if H is a Hamiltonian on a 1D lattice with first-neighbor interactions only, then its algebra contains all physically reasonable Hamiltonians of any range having translation symmetry. Section II treats the problem of extending the Green functions and DOS of H to the Green functions and DOS to H_e in the algebra generated by H. As an illustration of the general method, two Hamiltonians are treated for the 1D lattice, the first having second-

neighbor interactions and the second being of infinite range. These models are solved by extending from H for the nearest-neighbor case.

The second kind of extension is treated in Sec. III where Green functions and DOS for a pair of Hamiltonians H and K are extended to those of certain Hamiltonians defined on the Cartesian product of the lattices of H and K.

Let $V(H)$ represent the lattice that is the index set of H, and let $V(K)$ be the lattice of K. The Cartesian product of the two lattices is the set of pairs of index values such as (i,j), where $i \in V(H)$ and $j \in V(K)$. The square lattice, for example, is naturally represented as the Cartesian product of two linear chains. It should be recalled, however, that the lattice is only a set of sites. No connections or interactions between sites are implied until a Hamiltonian is defined.

The key for extending to Hamiltonians on the Cartesian product is again the use of transformations that preserve the eigenvectors. Thus in Sec. III we treat the extension of Green functions and DOS of H and K to Hamiltonians in the algebra generated by the pair of matrix direct products $H\otimes I$ and $I\otimes K$, where I stands for the identity on the lattice of K and H, respectively. Elements of this algebra are of the form

$$H_e = a_{00} I\otimes I + a_{10} H\otimes I + a_{01} I\otimes K + a_{11} H\otimes K + a_{20} H^2\otimes I + a_{02} I\otimes K^2 + \cdots = \sum_{m,n} a_{mn} H^m \otimes K^n \tag{3}$$

where the coefficients are real and the sum is over all independent powers of H and K. We refer to this as the product of the algebras of H and K. The subspace spanned by the first four terms in Eq. (3) has been treated in the context of graph theory of Cvetcović, Doob, and Sachs[10] and references cited.

As a first application, a study of nearest-neighbor Hamiltonians on the square and the simple cubic lattices is presented using results for the nearest-neighbor model on the linear chain. This includes a treatment of sites at boundaries of semiinfinite crystals, such as edge and corner sites of a square lattice.

A second example developed in Sec. IV involves a Sierpiński fractal lattice.[11,12] Alexander has computed Green functions for a nearest neighbor Hamiltonian on a Sierpiński lattice with perpendicular magnetic field.[13] We outlined the calculation by Alexander's renormalization method of Green functions for a slightly modified Sierpiński lattice with nearest-neighbor interactions. The results are extended to a second-neighbor model, and then to a nearest-neighbor Hamiltonian on a new fractal lattice that is more connected than the original Sierpiński lattice and has fractal dimension between 2 and 3. Possible spectral properties of such extensions are discussed in general terms.

As a final example, we again use the renormalization method in Sec. V to find the Green functions for a quasiperiodic Hamiltonian on a 1D lattice. The 1D Hamiltonian having strong or weak interactions between neighboring sites alternating in Fibonacci sequence[14] has been treated by several authors.[15,16] The calculation is extended to an exploration of the spectrum of Fibonacci quasiperiodic lattices in 2D and 3D. These admit inflation-deflation transformations, but do not have the interesting rotation symmetry of the Penrose lattice.[14]

A summary of the procedures and the results for the models treated is presented in Sec. VI.

II. EXTENSION TO HAMILTONIANS OF THE FORM $f(H)$

For a given H, the characteristic equation,

$$\sum_j H_{ij} u_{jv} = \alpha_v u_{iv} , \tag{4}$$

defines the set of normalized eigenvectors $\{u_v\}$ and the corresponding set $\{\alpha_v\}$ of eigenvalues that is the spectrum of H. The Green function $G_{ij}(z)$ is the i,j element of the resolvent matrix $G(z)$, as defined in Eq. (1), and it can be expressed as

$$G_{ij}(z) = \sum_v u_{iv} u_{jv}^* [z-\alpha_v]^{-1} . \tag{5}$$

The projected density of eigenvalues, or local density of states (LDOS) at site i will be defined[17] by

$$D_i(E) = \sum_v |u_{iv}|^2 \delta(E-\alpha_v) . \tag{6}$$

Since the eigenvectors are normalized, the sum over i of $D_i(E)$ yields the total DOS

$$D(E) = \sum_v \delta(E-\alpha_v) . \tag{7}$$

The objective is to extend the set $G(z)$ of Green functions and the LDOS and DOS for H, as expressed in Eqs. (5)–(7), to the corresponding quantities $G^{(e)}(z)$, $D_i^{(e)}(E)$, and $D^{(e)}(E)$ for H_e as defined in Eq. (2). The extension of $G(z)$ automatically gives an extension of the LDOS and DOS since, if η is a small positive number, Eq. (5) implies the approximate relation[18]

$$D_i(E) = -\frac{1}{\pi} \mathrm{Im}[G_{ii}(E+i\eta)] . \tag{8}$$

If η is small, the approximation in Eq. (8) replaces the delta functions in Eqs. (6) and (7) with Lorentzians of width η. This broadening is important in that it softens certain singularities that occur in the following development. That is to say, $\eta > 0$ moves the singularities off the real E axis.

However, it is also useful to have a simple formula for $D^{(e)}(E)$ directly in terms of $D(E)$, and this extension is easily derived. Thus a separate treatment is presented of the extension of the DOS and LDOS.

First consider the spectrum $\{\alpha_v^{(e)}\}$ of H_e. From Eq. (2),

$$\alpha_v^{(e)} = a_0 + a_1\alpha_v + a_2\alpha_v^2 + \cdots = \sum_n a_n \alpha_v^n = f(\alpha_v) . \tag{9}$$

The sequence of coefficients $\{a_n\}$ defining the function $f(x)$, which in turn defines the Hamiltonian H_e, may be freely chosen. Formally, $f(x)$ is a generating function[19] for the sequence, and the elements of the sequence are in-

dependent parameters of the Hamiltonian H_e.

For several reasons, it is usually sufficient to consider only a finite sequence of coefficients, so $f(x)$ becomes a polynomial. First, the range of H_e increases with the inclusion of higher powers of H, and interesting Hamiltonians normally are of shorter range. Second, if $V(H)$ contains a finite number N of sites, then there are not more than N independent powers of H.[20]

From Eq. (7) applied to H_e one has

$$D^{(e)}(E)=\sum_{\nu}\delta(E-f(\alpha_\nu)) \ . \tag{10}$$

Let $\{x_k(E)\}$ be the set of real zeros of $E-f(x)$ as a function of x. Then, if all the zeros were simple, one would have

$$\begin{aligned} D^{(e)}(E)&=\sum_{\nu}\sum_{k}\delta(x_k(E)-\alpha_\nu)[\,|f'(x_k(E))|\,]^{-1} \\ &=\sum_{k}D(x_k(E))[\,|f'(x_k(E))|\,]^{-1} \ . \end{aligned} \tag{11}$$

The E values at which a confluence of two or more roots causes denominators to vanish in terms on the right-hand side of Eq. (11) correspond to new Van Hove singularities of H_e, not inherited from H but rather introduced by the nonlinearity of the transformation of Eq. (2).

The new singularities are physical, but since they do not correspond to singularities in $D(E)$, they are not broadened by the damping parameter η of Eq. (8). To introduce broadening, the most natural procedure is to convolute the newly introduced features also with a Lorentzian of width η. This results in the integral

$$D^{(e)}(E)=\frac{\eta}{\pi}\int_{-\infty}^{\infty}D(x)\{[E-f(x)]^2+\eta^2\}^{-1}dx \ . \tag{12}$$

To avoid introducing another integration, Eq. (11) can be simply modified to soften the singularity. The method of introducing the damping is somewhat arbitrary to begin with, and the following is convenient. Define $\Gamma(x)$ by

$$\Gamma(x)=[(f'(x))^2+\eta^2]^{1/2} \tag{13}$$

then

$$D^{(e)}(E)=\sum_{k}D(x_k(E))[\Gamma(x_k(E))]^{-1} \ , \tag{14}$$

where the sum is over real roots.

The formula on the right-hand side of Eq. (11) is exact when there is no damping, i.e., when $\eta\to 0$. To insert damping, thus removing singularities in the DOS, there are three options. First, the Green functions of H can be extended by methods to be given presently, and these can in turn be used to get the LDOS via Eq. (8). Second, the smoothest extension directly from $D(E)$ to $D^{(e)}(E)$ is given by the integral of Eq. (12). When the forms of $D(x)$ and $f(x)$ are both simple enough, this integral can be done in closed form. When $D(x)$ is not given analytically, Eq. (12) can be done by numerical quadrature. Third, when $D(x)$ is given analytically, or is easily computed at arbitrary x, and the extension function $f(x)$ is more complicated, but with the real roots $\{x_k(E)\}$ easy to find, then the approximation of Eq. (14) may be more convenient than a numerical integral of Eq. (12).

One may wonder what advantage numerical integration of Eq. (12) would have over computing $D^{(e)}(E)$ by integrating directly over the band structure of H_e. If H_e has a band structure, then one advantage of Eq. (12), assuming $D(E)$ is known, is that it is always a 1D integration, while H_e may be defined on a 2D or 3D lattice. But a more important advantage of Eq. (12) is that it applies equally well to H_e without translation symmetry, thus *having* no band structure. Examples of such cases will be treated explicitly in the following sections.

Starting from Eq. (6), one can treat the LDOS in the same way. The weighting coefficients cause no new complication. It follows that $D_i(E)$ extends to $D_i^{(e)}(E)$ also by the same formulas. Thus to obtain $D_i^{(e)}(E)$, replace $D(x)$ by $D_i(x)$ in any one of Eqs. (11), (12), or (14).

Next consider the Green function $G_{ij}^{(e)}(z)$. In view of Eq. (5),

$$G_{ij}^{(e)}(z)=\sum_{\nu}u_{i\nu}u_{j\nu}^{*}[z-f(\alpha_\nu)]^{-1} \ . \tag{15}$$

Consider the function $F(s)=[z-f(s)]^{-1}$ where both z and s are complex. We restrict our attention to those choices of $f(s)$ such that $F(s)$ has the following properties. (a) $F(s)$ has no other singularities than poles, the positions of which are naturally functions of z. For most z values, we assume the poles are isolated and simple. (b) The behavior of $F(s)$ is such that there exists a sequence of circles of radii $\{r_p\}$ with $r_p\to\infty$, and with $|F(s)|<M$ whenever s is on a circle $|s|=r_p$ and with M independent of p. With these restrictions, $F(s)$ can be expanded in partial functions using a simple form of the Mittag-Leffler theorem.[21]

The expression for $G_{ij}^{(e)}(z)$ resulting when the Mittag-Leffler expansion is used for the denominators in Eq. (15) is

$$G_{ij}^{(e)}(z)=R(z)\delta_{ij}+\sum_{k}\frac{G_{ij}(s_k(z))}{f'(s_k(z))} \ , \tag{16}$$

where the sum is now over the set $\{s_k(z)\}$ of complex zeros of $z-f(s)$. If $f(x)$ is a polynomial or a rational function unbounded at infinity, then the residual $R(z)$ is zero. If $f(x)$ is a rational function having a finite value at infinity, then $R(z)$ is $F(s\to\infty)$. Otherwise, $R(z)$ is given by

$$R(z)=[z-f(0)]^{-1}+\sum_{k}[s_k(z)f'(s_k(z))]^{-1} \ . \tag{17}$$

Notice that in Eq. (16) the original Hamiltonian H contributes to $G_{ij}^{(e)}(z)$ only through the Green function $G_{ij}(s_k(z))$ in the numerator of each term in the sum. The rest of the formula is determined by $f(x)$. Singularities occur in individual summands for values of z such that poles coalesce, thus causing derivatives in the denominators to vanish. For functions $f(x)$ such that there is no residual $R(z)$, the coalescence of poles at a particular z represents a physical Van Hove singularity induced by the transformation from H to H_e. If there is a residual $R(z)$, then it cancels unphysical singularities that would

occur in the summation at z values such that a pole goes to infinity. The physical Van Hove singularities occur due to poles merging in the finite s plane. An example of the cancellation will be encountered below.

As an example of the use of the formalism, we treat 1D Hamiltonians with translation symmetry. The basic starting point is the set of Green functions for a nearest-neighbor model on a 1D chain

$$H_{mn}=\delta_{m+1,n}+\delta_{m-1,n} . \tag{18}$$

The Green functions also have translation symmetry, so we need only be concerned with the zeroth column of $G(z)$. In view of Eq. (1), $G(z)$ satisfies the matrix equation $[zI-H]G(z)=I$, whence

$$zG_{m0}(z)-G_{m+1,0}(z)-G_{m-1,0}(z)=\delta_{m0} . \tag{19}$$

The difference equation of Eq. (19) is conveniently solved using a generating function $g(x)$ defined by[19]

$$g(x)=\sum_m x^m G_{m0}(z) . \tag{20}$$

Multiplying Eq. (19) by x^m and summing on m yields

$$g(x)=\left[z-x-\frac{1}{x}\right]^{-1} \tag{21}$$

which is to be expanded in powers of x to obtain $\{G_{m0}\}$ as the coefficients. However, there are three different Laurent expansions in x, each with a different annulus of convergence. The physical solution is determined by the asymptotic boundary condition that $|G_{m0}|$ not diverge as $|m|\to\infty$. The annulus containing the unit circle $|x|=1$ is thus the proper choice. The expansion coefficients are

$$G_{m0}(z)=(z^2-4)^{-1/2}[q(z)]^{|m|} , \tag{22}$$

with $q(z)$ defined by

$$q(z)=\tfrac{1}{2}[z-(z^2-4)^{1/2}] , \tag{23}$$

and the branch cut is determined by choosing $(z^2-4)^{1/2}=(z-2)^{1/2}(z+2)^{1/2}$. The DOS at any site is found from Eq. (8). In the limit of zero damping, it is

$$D_0(E)=\frac{1}{\pi}(4-E^2)^{-1/2}\Theta(4-E^2) , \tag{24}$$

the unit step function Θ being 1 for positive argument and zero otherwise.

We first extend these results to the second-neighbor Hamiltonian treated by Davison and Levine[2]

$$(H_e)_{mn}=(\delta_{m+1,n}+\delta_{m-1,n})+b(\delta_{m+2,n}+\delta_{m-2,n}) . \tag{25}$$

Squaring H defined in Eq. (18) demonstrates that

$$H_e=bH^2+H-2bI . \tag{26}$$

Thus, the extension is generated by

$$f(s)=bs^2+s-2b , \tag{27}$$

so that characteristic roots of $z-f(s)$ are

$$s_\pm(z)=(2b)^{-1}\{-1\pm[1+4b(z+2b)]^{1/2}\} . \tag{28}$$

Therefore, the Green functions for the new model H_e are

$$G^{(e)}_{m0}(z)=\frac{[q(s_+(z))]^{|m|}}{[2bs_+(z)+1](s_+^2(z)-4)^{1/2}}+\frac{[q(s_-(z))]^{|m|}}{[2bs_-(z)+1](s_-^2(z)-4)^{1/2}} . \tag{29}$$

After some algebra, Eq. (29) can be shown to agree with Eq. (2.55) of Ref. 2. The corresponding DOS without damping follows from Eq. (11):

$$D_0^{(e)}(E)=\frac{1}{\pi}\frac{[4-s_+^2(E)]^{-1/2}}{2bs_+(E)+1}\Theta\left[\frac{1}{4b}-2b-E\right]\Theta(4-s_+^2(E))+\frac{1}{\pi}\frac{[4-s_-^2(E)]^{-1/2}}{2bs_-(E)+1}\Theta\left[\frac{1}{4b}-2b-E\right]\Theta(4-s_-^2(E)) . \tag{30}$$

We now proceed to outline the formal treatment of the general model with translation symmetry in 1D. If H_e has translation symmetry, then it is completely defined by the list $\{(H_e)_{m0}\}$ of elements in its zeroth column. For a translation symmetric H, the column-generating function $h(x)$ is defined by

$$h(x)=\sum_m x^m H_{m0} . \tag{31}$$

To obtain the column-generating function for H_e, multiply the mth element of the zeroth column of Eq. (2) by y^m and sum on m, taking advantage of the translation symmetry of H. The result is

$$h_e(y)=a_0+a_1h(y)+a_2h^2(y)+a_3h^3(y)+\cdots=f(h(y)) . \tag{32}$$

A formal solution for the function $f(x)$ can be found as follows. Let $x=h(y)$ and assume an inverse exists for some range of y. The inverse need not be single valued, any inverse will do. Thus let $y=h^{-1}(x)$. Then, formally,

$$f(x)=h_e(h^{-1}(x)) . \tag{33}$$

Choosing H defined in Eq. (18) as a base Hamiltonian, $h(y)=(y+1/y)$. For an inverse, one can choose the root

$$h^{-1}(x)=\tfrac{1}{2}[x+(x^2-4)^{1/2}] \quad (|x|>2) . \tag{34}$$

In fact, since H_e is Hermitian and translation symmetric, $h_e(-y)=h_e(y)$. Thus h_e must always be a function of $x=(y+1/y)$. A given term in the expansion of $h_e(y)$ can be paired with another to yield a contribution proportional to (y^p+y^{-p}) for some power p, which can in turn be expressed as a polynomial of degree p in $x=(y+1/y)$. Thus, if H_e is of finite range, $f(x)$ is a polynomial.

Having found $f(x)$, the next step is to find complex zeros $\{s_k(z)\}$ of $z-f(s)$. This may need to be done numerically, as with any method of finding $G_e(z)$. After computing $f'(s_k(z))$ at each $s_k(z)$, Eq. (17) gives Green functions for H_e. If $f(x)$ is a polynomial or a rational function with a pole at ∞, then only the last sum on the right-hand side of Eq. (17) contributes. Densities of states can be found by Eq. (11) from the real zeros when $z=E$ is real.

As a final example of this kind of extension, we consider a Hamiltonian H_e of infinite range having interaction strengths decrease exponentially with distance between sites:[22]

$$(H_e)_{m0}=\sum_{p=1}^{\infty}(\delta_{m,p}+\delta_{m,-p})b^{p-1} \tag{35}$$

where $|b|<1$. Hence $f(x)$ is not a polynomial;

$$\begin{aligned} h_e(y)&=y(1-by)^{-1}+\frac{1}{y}(1-b/y)^{-1} \\ &=\frac{(y+1/y)-2b}{1-b(y+1/y)+b^2} \end{aligned} \tag{36}$$

so

$$f(x)=(x-2b)/(1-bx+b^2) . \tag{37}$$

There is only one zero of $z-f(s)$.

$$s(z)=[(1+b^2)z+2b]/(bz+1) , \tag{38}$$

$$f'(s(z))=(bz+1)^2/(1-b^2) . \tag{39}$$

Because $f(s)$ has a finite value at $s=\infty$, there is a residual term $R(z)=b/(bz+1)$. Equation (16) gives

$$G_{m0}^{(e)}(z)=\frac{b}{bz+1}\delta_{m0}+\frac{(1-b^2)[q(s(z))]^{|m|}}{(bz+1)^2[s^2(z)-4]^{1/2}} . \tag{40}$$

This expression seems to have a pole at $z=-1/b$, which is independent of the nature of H. In fact, $G_{m0}^{(e)}(z)$ is well behaved at $z=-1/b$, the limit being

$$G_{m0}^{(e)}(-1/b)=\frac{b(1+b^2)}{1-b^2}\delta_{m0}-\frac{b^2}{1-b^2}H_{m0} \tag{41}$$

as can be seen by considering the corresponding limit of $F(s)$ directly. The H-independent singularity in the first term cancels with a singularity in the second term that occurs as $s(z)\to\infty$. This implies that $G_{m0}(z)$ must become independent of H as $z\to\infty$, which can be understood by examining the expression for the resolvent $G(z)$ in Eq. (1). Assuming the spectrum of H is bounded, then $G(z)\to Iz^{-1}$ as $z\to\infty$.

Thus, the extension of Green functions from a given H to those of H_e by Eq. (2) is provided by Eq. (16). The DOS or LDOS are extended directly using Eq. (11), or if broadening is required, by Eq. (12) or Eq. (14).

III. EXTENSION TO THE PRODUCT OF THE ALGEBRAS GENERATED BY H AND K

The main motivation for exploring the extension to Hamiltonians of the form of H_e in Eq. (3) is that the dimensionality of the lattice can be increased by this method.

As well as the eigenvalues $\{\alpha_\mu\}$ and the eigenvectors $\{u_\mu\}$ for Hamiltonian H, as defined in Eq. (4), suppose the eigenvalues $\{\beta_\nu\}$ and corresponding eigenvectors $\{v_\nu\}$ of another Hamiltonian K are also known. The lattices $V(H)$ and $V(K)$ may or may not be the same. Let pairs of index values such as (i,j) represent elements of the Cartesian product lattice. If A is an arbitrary matrix with index values from $V(H)$ and B is an arbitrary matrix with index values from $V(K)$, then the matrix elements of the direct product $(A\otimes B)$ are

$$(A\otimes B)_{(i,j)(k,l)}=(A_{ik})(B_{jl}) . \tag{42}$$

The eigenvectors $\{w_{\mu\nu}\}$ of H_e defined in Eq. (3) are the direct products of the eigenvectors of H and K, thus having components defined by

$$w_{(k,l)\mu\nu}=(u_{k\mu})(v_{l\nu}) . \tag{43}$$

And, in view of Eq. (3), the corresponding eigenvalues are given by

$$\gamma_{\mu\nu}^{(e)}=\sum_{m,n}a_{mn}\alpha_\mu^m\beta_\nu^n=f(\alpha_\mu,\beta_\nu) . \tag{44}$$

The function $f(x,y)$ introduced here is a generating function for the coefficients $\{a_{mn}\}$ of the transformation. We tentatively assume the singularities of $f(x,y)$ lie outside the spectra of H and K.

The total DOS can be extended in the following way. Let the symbols $D^{(H)}(E)$ and $D^{(K)}(E)$ represent the DOS for H and K. From Eq. (7), the DOS $D^{(e)}(E)$ for H_e is

$$\begin{aligned} D^{(e)}(E)&=\sum_{\mu,\nu}\delta(E-f(\alpha_\mu,\beta_\nu)) \\ &=\int_{-\infty}^{\infty}\left[\sum_\nu\delta(y-\beta_\nu)\right] \\ &\quad\times\left[\sum_\mu\delta(E-f(\alpha_\mu,y))\right]dy . \end{aligned} \tag{45}$$

Considering y as a parameter in the second factor one can express this symbolically as

$$D^{(e)}(E)=\int_{-\infty}^{\infty}D^{(f(H,y))}(E)D^{(K)}(y)dy , \tag{46}$$

where in view of the results Eq. (11) through Eq. (14) of Sec. II, $D^{(f(H,y))}(E)$ can be expressed in various ways. With no damping, Eq. (11) gives

$$D^{(f(H,y))}(E)=\sum_p \frac{D^{(H)}(x_p(y,E))}{|f_x(x_p(y,E),y)|} . \tag{47}$$

The set $\{x_p(y,E)\}$ in Eq. (47) is the set of real zeros in x of the function $E-f(x,y)$ with real parameters y and E. In the denominators, $f_x(x,y)$ indicates the partial derivative $\partial f(x,y)/\partial x$. To include damping, and thus to remove the potentially problematic singularities from the integrand of Eq. (46), the method presented in Eqs. (13) and (14) can be used. With finite broadening η in both $D^{(H)}(x)$ and $D^{(K)}(y)$, we replace the denominators of Eq. (47) by modified denominators of the form

$$\Gamma_p(y,E)=[f_x^2(x_p(y,E),y)+\eta^2]^{1/2} . \tag{48}$$

Because the vector coefficients carry through the steps of the derivation given for the DOS leading to Eq. (46) and Eq. (47), the LDOS satisfy similar expressions. To obtain the LDOS at site (i,j) for Hamiltonian H_e, replace $D^{(e)}(E)$ by $D^{(e)}_{(i,j)}(E)$ and $D^{(H)}(x)$ and $D^{(K)}(y)$ by $D_i^{(H)}(x)$ and $D_j^{(K)}(y)$, respectively in Eqs. (46) and (47). Thus these equations give an extension of the DOS and LDOS for H and K to the corresponding functions for H_e belonging to the algebra generated by $H\otimes I$ and $I\otimes K$.

A formal extension of the Green functions also results from a development similar to that of the section above. The Green functions for H and K are assumed known. The Green function for H between sites i and j is denoted by $G_{ij}^{(H)}(z)$, while that for K between sites k and l is $G_{kl}^{(K)}(z)$. For the extension to H_e, one has

$$\begin{aligned} G^{(e)}_{(i,j)(k,l)}(z)&=\sum_{\mu,\nu} w_{(i,j)\mu\nu}w^*_{(k,l)\mu\nu}[z-f(\alpha_\mu,\beta_\nu)]^{-1} \\ &=\sum_{\mu,\nu} u_{i\mu}v_{j\nu}u^*_{k\mu}v^*_{l\nu}[z-f(\alpha_\mu,\beta_\nu)]^{-1} . \end{aligned} \tag{49}$$

Factoring the summation of Eq. (49) requires an integration device to play a role similar to the role played by $D^{(K)}(y)$ in Eq. (46). Such a device is obtained by examination of Eq. (5). If one approximates the delta functions by Lorentzians, one has for small positive η,

$$-\frac{1}{\pi}\mathrm{Im}[G_{jl}^{(K)}(y+i\eta)]=\sum_\nu v_{i\nu}v^*_{l\nu}\delta(y-\beta_\nu) . \tag{50}$$

Thus

$$G^{(e)}_{(i,j)(k,l)}(z)=-\frac{1}{\pi}\int_{-\infty}^{\infty}\mathrm{Im}[G_{jl}^{(K)}(y+i\eta)]\left[\sum_\mu u_{i\mu}u^*_{k\mu}[z-f(\alpha_\mu,y)]^{-1}\right]dy . \tag{51}$$

Again applying the results of the previous section with y considered as a parameter in the second factor of Eq. (51) yields the formal expression

$$G^{(e)}_{(i,j)(k,l)}(z)=-\frac{1}{\pi}\int_{-\infty}^{\infty}\mathrm{Im}[G_{jl}^{(K)}(y+i\eta)]G_{ik}^{(f(H,y))}(z)dy , \tag{52}$$

where, using Eq. (16),

$$G_{ik}^{(f(H,y))}(z)=R(y,z)\delta_{ik}+\sum_p \frac{G_{ik}^{(H)}(s_p(y,z))}{[f_s(s_p(y,z),y)]} , \tag{53}$$

the sum being over all complex poles $\{s_p(y,z)\}$ of $F(s)=[z-f(s,y)]^{-1}$. Equation (53) holds at values of real y and complex z such that the poles of $F(s)$ are simple and isolated. The discussion regarding $R(z)$ in Eqs. (16) and (17) applies here to the residual term $R(y,z)$, y being considered a parameter.

For an arbitrary H_e defined in the manner of Eq. (3), the formulas in Eq. (46) and Eq. (52) give at least formal expressions for the DOS and the Green functions. To illustrate, we find an integral formula for the Green functions of a model on a square lattice with first-, second-, and third-neighbor matrix elements 1, a and b:

$$\begin{aligned} (H_e)_{(m,n)(0,0)}&=(\delta_{m,1}+\delta_{m,-1})\delta_{n,0}+\delta_{m,0}(\delta_{n,1}+\delta_{n,-1}) \\ &\quad +a(\delta_{m,1}+\delta_{m,-1})(\delta_{n,1}+\delta_{n,-1})+b[(\delta_{m,2}+\delta_{m,-2})\delta_{n,0}+\delta_{m,0}(\delta_{n,2}+\delta_{n,-2})] . \end{aligned} \tag{54}$$

Using H of Eq. (18) as a base Hamiltonian,

$$\begin{aligned} H_e&=I\otimes H+H\otimes I+aH\otimes H+bI\otimes(H^2-2I)+b(H^2-2I)\otimes I \\ &=-4bI\otimes I+I\otimes H+H\otimes I+aH\otimes H+bH^2\otimes I+bI\otimes H^2 . \end{aligned} \tag{55}$$

The function $f(x,y)$ generating the transformation is

$$f(x,y)=-4b+x+y+axy+bx^2+by^2 . \tag{56}$$

The roots of $z-f(s,y)$ are therefore

$$s_\pm(y,z)=(2b)^{-1}[-(ay+1)\pm[A(y,z)]^{1/2}] , \tag{57}$$

where the discriminant $A(y,z)$ is

$$A(y,z)=(a^2-4b^2)y^2-2(2b-a)y+(16b^2+4bz+1)\ . \tag{58}$$

Thus the integral expression for the Green functions is

$$G^{(e)}_{(m,n)(0,0)}(z)=-\frac{1}{\pi}\int_{-\infty}^{\infty}\mathrm{Im}[G^{(H)}_{n0}(y+i\eta)][A(y,z)]^{-1/2}[G^{(H)}_{m0}(s_+(y,z))-G^{(H)}_{m0}(s_-(y,z))]dy\ . \tag{59}$$

Expressions for the Green functions for H are given in Eq. (22).

Singularities of the integrands are apt to occur along the real y axis that is the integration contour in Eq. (46) and Eq. (52). They may be integrable, as are the singularities of $D^{(K)}(y)$ in Eq. (46), or they may be nonintegrable. Indeed, the occurrence of nonintegrable singularities in the integrands is the mechanism by which Van Hove singularities of K and $f(H,y)$ are transmitted to H_e. In the case of branch points, care must be taken to keep the integrand on a consistent sheet of the y plane. In Eq. (59), for example, this requires two precautions. First, the root functions occurring in the definition of $G^{(H)}$ must be cut as in the discussion following Eq. (22). Then, the function $[A(y,z)]^{1/2}$ must be cut as follows:

$$[A(y,z)]^{1/2}=(a^2-4b^2)^{1/2}(y-y_+(z))^{1/2}(y-y_-(z))^{1/2}\ , \tag{60}$$

$$y_\pm(z)=(a^2-4b^2)[(2b+a)\pm[B(z)]^{1/2}]\ , \tag{61}$$

with

$$B(z)=4b(2b-a)[1+4b(2b+a)+(2b+a)z]\ . \tag{62}$$

With these conventions, Eq. (59) can be integrated numerically. However, as $f(x,y)$ becomes more complicated, the choice of branch cuts becomes more difficult.

For a certain set of special cases, the formulation simplifies quite a bit. If $H_e=H\otimes I+I\otimes K$, so that $f(x,y)=x+y$, then the extension integrals Eq. (46) and Eq. (52) become convolutions. An extension theory for eigenvalues is developed in Ref. 10 for special cases of this sort. One sees formally that $G^{(H+y)}(z)=G^{(H)}(z-y)$ and $D^{(H+y)}(E)=D^{(H)}(E-y)$. Thus the integral formulas are

$$D^{(e)}(E)=\int_{-\infty}^{\infty}D^{(H)}(E-y)D^{(K)}(y)dy\ , \tag{63}$$

$$G^{(e)}_{(i,j)(k,l)}(z)=-\frac{1}{\pi}\int_{-\infty}^{\infty}\mathrm{Im}[G^{(K)}_{jl}(y+i\eta)]G^{(H)}_{ik}(z-y)dy\ . \tag{64}$$

As an example consider a simple square lattice Hamiltonian with nearest-neighbor elements $+1$.

$$H^{(e)}_{(m,n)(0,0)}=(\delta_{m,1}+\delta_{m,-1})\delta_{n,0}+\delta_{m,0}(\delta_{n,1}+\delta_{n,-1})\ , \tag{65}$$

$$H^{(e)}=I\otimes H+H\otimes I\ . \tag{66}$$

where the base Hamiltonian is again that of Eq. (18). The Hamiltonian of Eq. (65) reduced to a finite lattice is treated as an example in Ref. 10. Morita has expressed its Green functions on the infinite lattice in terms of complete elliptic integrals by solving directly the difference equations implied by Eq. (1).[7]

Figure 1(a) shows the result for $D^{(e)}_{(0,0)}(E)$ obtained by direct numerical convolution as prescribed by Eq. (63) with both factors in the integrand obtained from Eq. (24). The integral can also be done in closed form. On using Eq. (24) for the integrand in Eq. (63), and assuming E is in the range $0<E<4$,

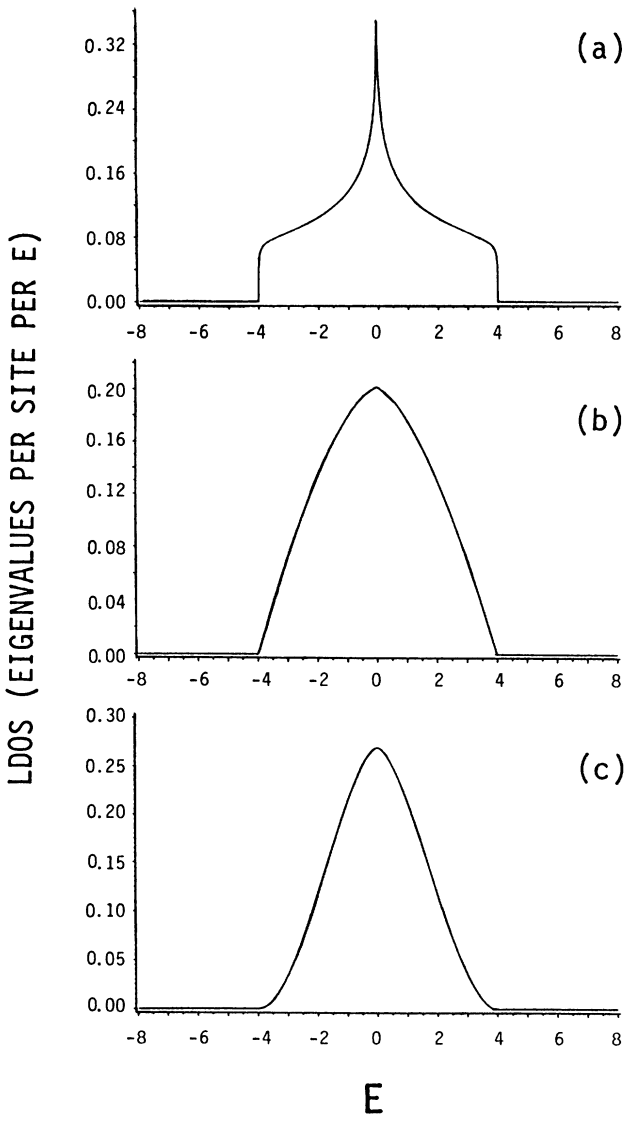

FIG. 1. LDOS for square lattice. (a) Typical site of infinite lattice. (b) Site at edge, far from corner, on semiinfinite lattice. (c) Corner site.

$$D^{(e)}_{(0,0)}(E)=\frac{1}{\pi^2}\int_{E-2}^{2}\frac{1}{[(4-x^2)(4-(E-x)^2)]^{1/2}}dx$$
$$=\frac{4}{\pi^2(4+E)}K((4-E)/(4+E))\ , \qquad (67)$$

with $K(u)$ the complete elliptic integral of the first kind. The DOS is symmetric, and is zero outside the range $|E|<4$.

For the Green function $G^{(e)}_{(0,0)(0,0)}(z)$, the integrand factors for Eq. (64) are provided by Eq. (24) and Eq. (22). Thus, choosing the phase of the integrand zero for z real and >4,

$$G^{(e)}_{(0,0)(0,0)}(z)=\frac{1}{\pi}\int_{-2}^{2}\frac{1}{[(4-x^2)((z-x)^2-4)]^{1/2}}dx$$
$$=\frac{2}{\pi z}K(4/z)\ . \qquad (68)$$

Analytic continuation[7] together with the Landen identity[23] recovers Eq. (67) from Eq. (68) via Eq. (8).

Due to translation symmetry, an arbitrary Green function for the square lattice Hamiltonian of Eq. (65) reduces to the form $G^{(e)}_{(m,n)(0,0)}(z)$. It is clear that this can be expressed in terms of complete elliptic integrals, since the integrand of

$$G^{(e)}_{(m,n)(0,0)}(z)=-\frac{1}{\pi}\int_{-\infty}^{\infty}\mathrm{Im}\left[\frac{[q(x+i\eta)]^{|m|}}{[(x+i\eta)^2-4]^{1/2}}\right]\left[\frac{[q(z-x)]^{|n|}}{[(z-x)^2-4]^{1/2}}\right]dx \qquad (69)$$

is a rational function of x and of the square roots of the two quadratic functions x^2-4 and $(z-x)^2-4$.

To see the utility of the formalism in cases where there is no translation symmetry it is interesting to treat a semiinfinite square lattice. One can imagine a square lattice with points indexed by $\{(k,l)\}$ covering only the half plane $l>0$, or the quarter plane $l>0$, $k>0$. To treat a square lattice with edges and corners, the necessary tool is the base Hamiltonian K for a semiinfinite line. Let K_{ln} be given by Eq. (18) when both l and n are >0, and let it be zero otherwise.

A convenient way of getting $G^{(K)}(z)$ from $G^{(H)}(z)$ is given by Freeman.[24] A barrier potential V is introduced on site 0 in the linear chain Hamiltonian H of Eq. (18). The Green functions of K are the Green functions of $H+V$ in the limit of large V, when the site indices are positive. One finds

$$G^{(K)}_{ln}(z)=G^{(H)}_{ln}(z)-G^{(H)}_{l0}(z)[G^{(H)}_{00}(z)]^{-1}G^{(H)}_{0n}(z)$$
$$=(z^2-4)^{-1/2}\{[q(z)]^{|l-n|}-[q(z)]^{l+n}\}\ , \qquad (70)$$

where the indices are restricted to be positive. The LDOS are thus given by

$$D^{(K)}_{l}(E)=D^{(H)}_{0}(E)[1-T_{2l}(\tfrac{1}{2}E)]\ , \qquad (71)$$

with $T_l(x)$ the lth Chebyshev polynomial $\cos[l\cos^{-1}(x)]$.[3]

A complete study of the square lattice proceeds as follows. Sites far from any boundary are most easily treated using the Hamiltonian of Eq. (65), which we now call H_0. Thus, $H_0=H\otimes I+I\otimes H$. To study sites near an edge, but far from a corner, we form $H_1=H\otimes I+I\otimes K$, and to study sites near a corner $H_2=K\otimes I+I\otimes K$.

The LDOS for an edge site, $D^{(1)}_{(0,1)}(E)$, is computed by using $D^{(H)}_0(E-x)$ from Eq. (24) and $D^{(K)}_1(x)$ from Eq. (71) in the integrand of Eq. (63). The result of numerical convolution for $D^{(1)}_{(0,1)}(E)$ is shown in Fig. 1(b). The LDOS for a corner site, $D^{(2)}_{(1,1)}(E)$ shown in Fig. 1(c), is obtained using $D^{(K)}_1(x)$ and $D^{(K)}_1(E-x)$ in Eq. (63). Notice that $D^{(1)}_{(0,1)}(E)$ corresponds to $D^{(2)}_{(\infty,1)}(E)$. Green functions can likewise be found using Eq. (64).

All of the integrals encountered in the calculation of Green functions and DOS for H_0, H_1, and H_2 can be done in closed form, for the reason mentioned in connection with Eq. (69). From examination of the integrand in Eq. (63), with factors $D^{(H)}(E-y)$ and $D^{(K)}(y)$ selected arbitrarily from either Eq. (24) or Eq. (71), it is clear it will be a rational function of x and of the square roots of $4-x^2$ and $4-(E-x)^2$. Thus the LDOS can be expressed as a combination of complete elliptic integrals. A similar consideration of the integrand of Eq. (64) shows that the Green functions can also be so expressed. We have demonstrated that all Green functions and DOS for a semiinfinite square lattice Hamiltonian with nearest-neighbor matrix elements can be expressed in closed form in terms of complete elliptic integrals.

A similar study of a semiinfinite cubic lattice is shown in Fig. 2. A nearest neighbor Hamiltonian for the cubic lattice is $H_3=H\otimes I\otimes I+I\otimes H\otimes I+I\otimes I\otimes H$. To include surfaces, edges and a corner, one also needs $H_4=H\otimes I\otimes I+I\otimes H\otimes I+I\otimes I\otimes K$, $H_5=H\otimes I\otimes I+I\otimes K\otimes I+I\otimes I\otimes K$, and $H_6=K\otimes I\otimes I+I\otimes K\otimes I+I\otimes I\otimes K$. Figure 2(a) shows $D^{(3)}_{(0,0,0)}(E)$ for a typical site far from any boundary. The curve is obtained by numerical integration of Eq. (63). Noting that $H_3=H_0\otimes I+(I\otimes I)\otimes H$, one substitutes $D^{(0)}_{(0,0)}(x)$ obtained for the square lattice and $D_0(E-x)$ from Eq. (24) into Eq. (63). The three curves in Fig. 2(b) represent $D^{(4)}_{(0,0,1)}(E)$, $D^{(5)}_{(0,1,1)}(E)$, and $D^{(6)}_{(1,1,1)}(E)$ for sites at a surface, edge and corner, corresponding to the lettering A, B, and C. The Green functions are also obtained by this decomposition via Eq. (64).

Morita and Horiguchi[5] have expressed Green functions for H_3 in terms of sums of simple integrals of complete elliptic integrals. Since we see that each LDOS for any of H_3 through H_5 can be expressed by an integral in Eq. (63) that is a convolution of a complete elliptic integral (from the square lattice calculation) and either $D^{(H)}_0(x)$ or $D^{(K)}(x)$, which contain at most rational functions of x

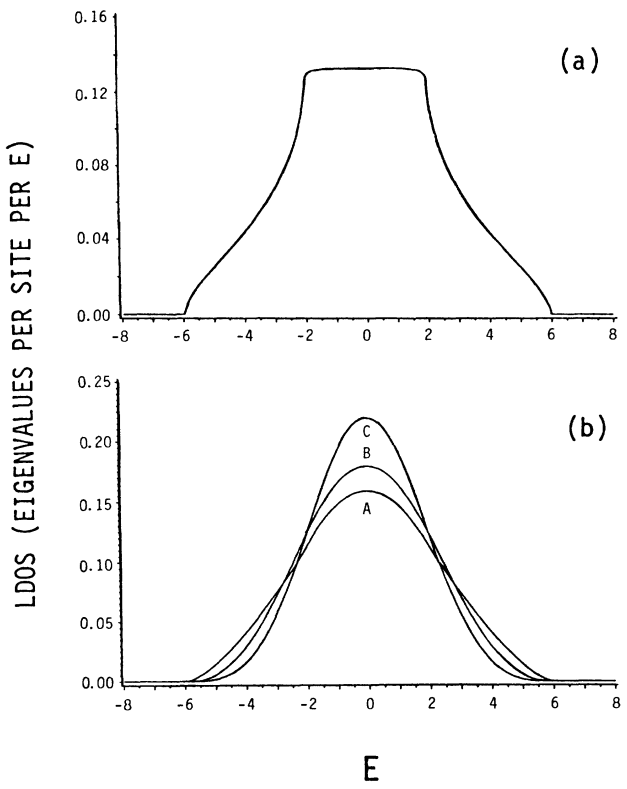

FIG. 2. LDOS for simple cubic lattice. (a) Typical site of infinite lattice. (b) Curves A,B,C for sites at surface, edge, and corner.

and $(4-x^2)^{1/2}$, we can say all LDOS on the semiinfinite cubic lattice are relatively simple integrals involving sums of elliptic integrals. So are the Green functions.

In closing this section a limitation of the method is noted. In 1D, the general H_e can be expressed quite easily in terms of the basic H. This is because the fact that H_e is Hermitian and translation-symmetric forces its column generating function $h_e(u)$ to be a function quite naturally of $u+1/u$. The situation for H_e with translation symmetry in higher dimensions is not so fortunate.

Let the column-generating function $h_e(u,v)$ be defined by

$$h_e(u,v)=\sum_{m,n} H^{(e)}_{(m,n)(0,0)} u^m v^n \ . \tag{72}$$

Following the steps outlined above in the 1D case, one has

$$h_e(u,v)=f(h(u),k(v)) \ , \tag{73}$$

where $h(u)$ and $k(v)$ generate columns of H and K, respectively. Thus the formal expression for $f(x,y)$ is

$$f(x,y)=h_e(h^{-1}(x),k^{-1}(y)) \ . \tag{74}$$

However, unless H_e is symmetric with respect to both $n\rightarrow -n$ and $m\rightarrow -m$ separately, thus having essentially rectangular symmetry, the expression for $f(x,y)$ in Eq. (74) does not have the properties necessary in order to use the Mittag-Leffler expansion producing Eq. (53).

As an illustration of this kind of failure, consider the triangle lattice Hamiltonian

$$(H_e)_{(m,n)(0,0)}=(\delta_{m,1}+\delta_{m,-1})\delta_{n,0}+\delta_{m,0}(\delta_{n,1}+\delta_{n,-1}) +(\delta_{m,1}\delta_{n,-1}+\delta_{m,-1}\delta_{n,1}) \ , \tag{75}$$

$$h_e(u,v)=(u+1/u)+(v+1/v)+(u/v+v/u) \ , \tag{76}$$

thus, applying Eq. (34) in Eq. (74) yields

$$f(x,y)=x+y+\tfrac{1}{2}xy-\tfrac{1}{2}(x^2-4)^{1/2}(y^2-4)^{1/2} \ . \tag{77}$$

Although $f(x,y)$ has a Laurent expansion near $x=0$, $y=0$, it has branch points. Thus Eq. (47) and Eq. (53) do not apply. In retrospect, one should realize the transformation of Eq. (3) preserves rectangular symmetry. However lattices with hexagonal symmetry in 3D, for example, can be reached by starting from a 2D lattice with hexagonal symmetry.

The strength of the current method lies in its applicability to lattice Hamiltonians *without* translation symmetry. In the following sections, we take up two examples of such Hamiltonians.

IV. FRACTAL LATTICES

The sequence of graphs in Fig. 3 represents a sequence of nearest-neighbor lattice Hamiltonians, the vertices representing lattice sites and the edges representing nonvanishing Hamiltonian matrix elements. Any graph in the sequence is obtained by connecting together three copies of the previous one. Taking a single vertex as the zeroth generation, then the nth generation has $N=3^n$ lattice sites and the length of one side of the graph is $L\sim 2^n$. Thus, as the sequence progresses, the graphs become self similar and approximate a Sierpiński fractal with fractal dimension[11] $\bar{d}=\ln 3/\ln 2$. The sixth graph is shown in Fig. 4(a). We refer to the the nth graph in this sequence, or to the corresponding lattice Hamiltonian, as the nth generation threefold coordinated Sierpiński lattice, since each site except the corner site has three neighbors.

Such hierarchical families of lattices are well studied. Eigenvalues of related fourfold Sierpiński lattices have been found by Domany, Alexander, Bensimon, and Kadanoff[12] using a decimation procedure. The Green functions of the fourfold case have been found by Alexander.[13]

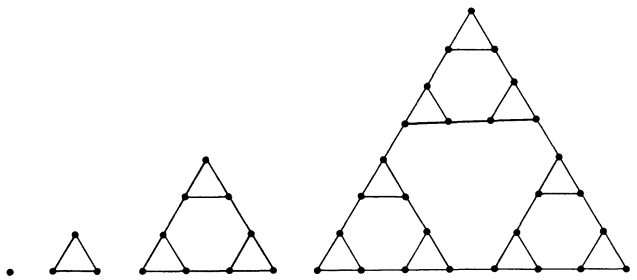

FIG. 3. Graphs representing generations 0, 1, 2, and 3 in sequence of Sierpiński lattice Hamiltonians.

The threefold coordinated Sierpiński lattice, as illustrated in Fig. 4(a) has been studied by O'Shaughnessy and Procaccia[25] who show that, like the fourfold case, it has spectral dimension, or fracton dimension, $\bar{\bar{d}}=2(\ln 3)/\ln 5$. The spectral dimension[26] is the dimension of an effective wave vector space such that $D(E)\,|\,dE\,| \propto d^{\bar{\bar{d}}}k$, when E approaches the maximum eigenvalue E_0. In the current case, $E_0=+3$. Thus, with $|E-E_0|\sim k^2$, one would expect $D(E)\propto |E-E_0|^c$ where $c=(\frac{1}{2}\bar{\bar{d}}-1)$. More generally, there should be an α such that $D(E_0-\alpha\,\Delta E)\approx\alpha^c D(E_0-\Delta E)$ for ΔE small enough.[27]

For an arbitrary graph of the sequence implied by Fig. 3, the corresponding Hamiltonian H is defined as follows. Whenever sites m and n are connected by an edge, $H_{mn}=+1$, otherwise $H_{mn}=0$. In Fig. 4(b), the subgraphs A, B, and C represent three copies of generation n. When connected as shown, the $(n+1)$th generation results.

Certain Green functions for the threefold Sierpiński lattice are now computed using Alexander's synthetic method.[13] It is a renormalization method insofar as one constructs a recursion between two consecutive Hamiltonians of the sequence. The strategy is to express Green functions of the $(n+1)$th generation in terms of the corresponding ones on the nth, and so by induction to solve for some subset of Green functions on the entire sequence of lattice Hamiltonians.

We therefore consider Fig. 4(b). By H_0 we denote the matrix corresponding to the disconnected subgraphs A, B, and C. So H_0 is the direct sum of three copies of the nth Hamiltonian. The sparse matrix V connects the blocks A, B, and C to form the $(n+1)$th Hamiltonian H:

$$H=H_0+V\ . \tag{78}$$

The desired Green functions are elements of the resolvent

$$G(z)=[zI-H]^{-1}\ . \tag{79}$$

It is assumed that the necessary Green functions are known; thus we know the necessary elements of

$$g(z)=[zI-H_0]^{-1}\ . \tag{80}$$

Substituting Eq. (78) into Eq. (79) and rearranging, one has

$$G(z)=g(z)+g(z)VG(z)\ , \tag{81}$$

which is the principal formula giving recursion relations between generations in any such hierarchy of Hamiltonians.

Since the subgraphs of Fig. 4(b) connect to one another only at their corners, a recursion should exist involving only two distinct Green functions on each generation, namely, the corner-to-same-corner Green function and the corner-to-other-corner Green function. On the nth generation subgraph, these are respectively such functions as $g_{ll}(z)$ or $g_{mm}(z)$, which we call $g_0(z)$, and such functions as $g_{lm}(z)$ or $g_{nr}(z)$, which we call $g_1(z)$. These correspond on the next generation to functions such as $G_{ll}(z)$, which we call $G_0(z)$, and $G_{pl}(z)$ which we call $G_1(z)$.

To get a recursion for $G_0(z)$, $G_{ll}(z)$ is first computed using Eq. (81)

$$\begin{aligned}G_{ll}(z)&=g_{ll}(z)+g_{lm}(z)V_{mn}G_{nl}(z)+g_{lq}(z)V_{qs}G_{sl}(z)\\&=g_0(z)+2g_1(z)G_{nl}(z)\ .\end{aligned} \tag{82}$$

Next, $G_{nl}(z)$ is computed, and so on, resulting in a set of equations

$$G_{nl}(z)=g_0(z)G_{ml}(z)+g_1(z)G_{rl}(z)\ , \tag{83}$$

$$G_{ml}(z)=g_1(z)+[g_0(z)+g_1(z)]G_{nl}(z)\ , \tag{84}$$

$$G_{rl}(z)=g_0(z)G_{rl}(z)+g_1(z)G_{ml}(z)\ . \tag{85}$$

Equations (82)–(85) are solved for $G_{ll}(z)$ in terms of $g_0(z)$ and $g_1(z)$. To find $G_{pl}(z)$, one more equation is needed:

$$G_{pl}(z)=g_1(z)[G_{ml}(z)+G_{rl}(z)]\ . \tag{86}$$

The notation is simplified by introducing $x=g_0(z)$, $y=g_1(z)$ and the corresponding symbols $X=G_0(z)=G_{ll}(z)$ and $Y=G_1(z)=G_{pl}(z)$. Solving simultaneously yields the recursion relations

$$X=F_1(x,y)=x+\frac{2y^2(x-x^2+y^2)}{(1-x-y)(1-x^2+y+y^2)}\ , \tag{87}$$

$$Y=F_2(x,y)=\frac{y^2(1-x+y)}{(1-x-y)(1-x^2+y+y^2)}\ . \tag{88}$$

Thus starting with a single site as the zeroth Hamiltonian, for which $x=y=1/z$, iteration of Eqs. (87) and (88)

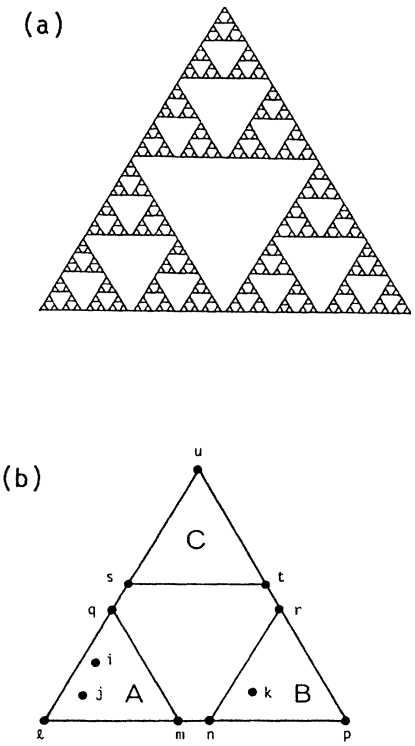

FIG. 4. Sierpiński hierarchical lattice Hamiltonian. (a) Graph for generation 6. (b) Construction of generating $n+1$ by connecting graphs A, B, and C corresponding to generation n.

produces the pair of corresponding Green functions for each lattice Hamiltonian in the sequence. We note in passing that starting with a different zeroth Hamiltonian, such as that of a sixfold ring, defines another sequence of Hamiltonians connected by the same recursion formulas.

The planar map $(x,y)\rightarrow(X,Y)$ of Eqs. (87) and (88) has a line of stable fixed points for $y=0$ and an unstable fixed point at $x=-\frac{1}{3},y=+\frac{2}{3}$. The line $x+y=1$ and the hyperbola $4x^2-(2y+1)^2=3$ go into infinity. The two lines $x+2y=1$ and $y-x=1$ are invariant in the sense that any point on one of these lines goes into another point on the same line. These invariant lines intersect at the unstable fixed point. The line $x-y=1$ maps directly into the fixed point $x=1,y=0$.

Along $x+2y=1$, the recursion reduces to $Y=(3y)/(5-3y)$, so at the point $x=1,y=0,y\sim(\frac{3}{5})^N$. Likewise for the line $y-x=1$, the recursion becomes $Y=y/[3(y-1)]$, and so $y\sim(-\frac{1}{3})^N$ near $x=-1,y=0$.

The LDOS for a corner site is computed using the recursion of Eqs. (87) and (88). We let $z=E+i\eta$ for small positive η and start with $x=y=1/z$. Equations (87) and (88) are iterated n times to get X for the nth generation. The LDOS is obtained directly from $-\mathrm{Im}[X]/\pi$.

Figure 5 is the LDOS for the corner site at $n=20$ iterations for various ranges of E. The energy resolution of each curve is limited by η to be a constant fraction, about $\frac{1}{250}$, of the range shown. Thus η decreases from curve to curve to maintain constant relative resolution. Since the area under each peak in the LDOS corresponding to an individual eigenstate remains fixed, the peak height is magnified proportionately as the scale becomes finer.

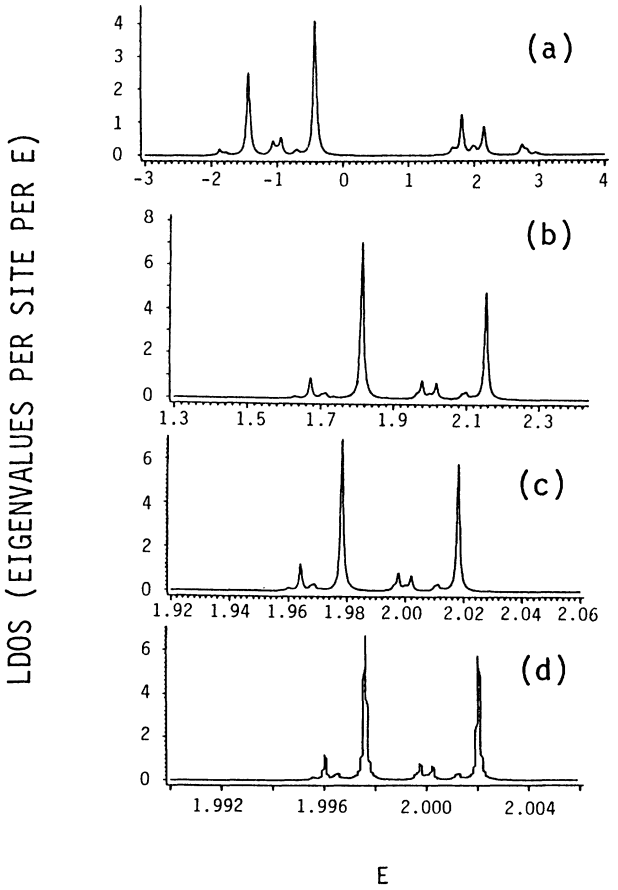

FIG. 5. LDOS of corner site l near $E=+2$. (a) Entire spectrum, (b) through (d) successive enlargements at higher resolution showing self similarity close to $E=+2$.

The complete spectrum shown in Fig. 5(a) extends from -2 to $+3$. It has been shown for the fourfold case[12] that the spectrum contains no continuum. In any open interval there are gaps containing no eigenvalues. The curves presented in Fig. 5 for the threefold case are consistent with this. One expects the fine structure, which depends on large length scales, to have similar properties in the three and fourfold cases.

Figures 5(b)–5(d) illustrate self-similarity of the LDOS near $E=+2$. This self-similarity is also typical of hierarchical lattices and is analyzed in Ref. 12. Self similarity of the clustering of eigenvalues near $E_0=+3$ is demonstrated in Fig. 6. An E scale reduction of $\frac{1}{5}$ results[12] in an approximately similar LDOS. In successive curves, the height of the peak at lowest E for each cluster increases slightly, while the other peaks decrease slightly in height. The area ratio is thus quite near $\frac{1}{5}$ also. Hence the scaling exponent p defined by

$$D_l(E_0-\tfrac{1}{5}\Delta E)\approx(\tfrac{1}{5})^p D_l(E_0-\Delta E)\ , \tag{89}$$

for small enough ΔE, is close to $+1$. The discrepancy between p and the exponent $c=\frac{1}{2}\bar{d}-1$ for the total DOS is due to the inclusion in Eq. (6) of squared vector coefficients to the definition of the LDOS. Both p and c are of concern when the results for the Sierpiński model are extended to Hamiltonians with higher dimensional lattices.

The lattice Hamiltonian H of Fig. 4 is first extended to a second-neighbor Hamiltonian on the same lattice. This requires some preliminary adjustment of H. As specified above, the sites of H are threefold coordinated, except that the corner sites are twofold. To make H uniformly threefold coordinated, the corner sites can be connected to corresponding sites on another copy of the same lattice with the same H.[12] Alternatively, the LDOS can be examined for sites far from a corner, such as site m of Fig. 4.

A representative site 0 of a uniformly threefold Hamiltonian is illustrated in Fig. 7. Nearest-neighbor sites are 1, 2, and 3 while second neighbor sites are 4, 5, 6, and 7. Thus

$$H_{m,0}=\delta_{m,1}+\delta_{m,2}+\delta_{m,3}\ . \tag{90}$$

It is interesting to add a second-neighbor term H_2 and study $H+bH_2$ where

$$[H+bH_2]_{m,0}=(\delta_{m,1}+\delta_{m,2}+\delta_{m,3}) +b(\delta_{m,4}+\delta_{m,5}+\delta_{m,6}+\delta_{m,7})\ . \tag{91}$$

Unfortunately, H_2 is not in the algebra generated by H. Therefore, we select a different base Hamiltonian defined by making another adjustment to H.

Let H_1 be defined on the lattice of H. The matrix elements of H_1 are either 0 or 1 or b. If H_{mn} is zero, then

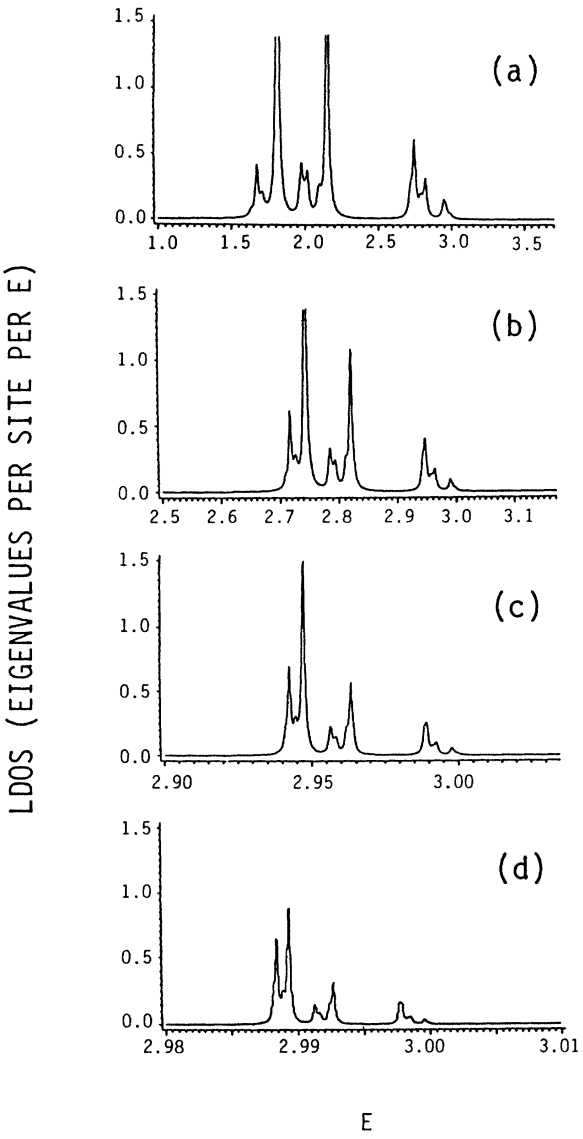

FIG. 6. LDOS of corner site near $E=+3$. Successive enlargements (b) through (d) show scaling at $E_0=+3$.

$(H_1)_{mn}$ is zero. The nonzero elements of H_1 are b if they correspond to edges of one of the generation-1 triangles, and they are 1 otherwise. Thus, from Fig. 7,

$$(H_1)_{m,0}=\delta_{m,1}+b(\delta_{m,2}+\delta_{m,3}) . \tag{92}$$

One finds that

$$\begin{aligned}(H_1^2+H_1)_{m,0}=&(1+2b^2)\delta_{m,0}+\delta_{m,1}\\&+b(1+b)(\delta_{m,2}+\delta_{m,3})\\&+b(\delta_{m,4}+\delta_{m,5}+\delta_{m,6}+\delta_{m,7}) .\end{aligned} \tag{93}$$

The second and third term combine to form H of Eq. (90) if $b^2+b-1=0$. Thus, the one parameter family in Eq. (91) intersects the algebra of H_1 at two points, $b=\tau$, or $b=-1/\tau$, where $\tau=\frac{1}{2}(5^{1/2}-1)$ is the Fibonacci ratio. We choose $b=\tau$.

$$H_1^2+H_1-(1+2\tau^2)I=H+\tau H_2 , \tag{94}$$

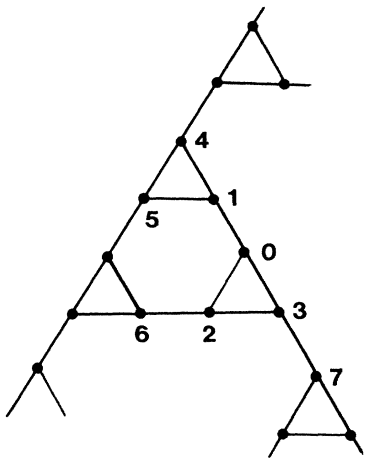

FIG. 7. Representative sites of uniformly threefold lattice. First neighbors of site 0, are 1, 2, and 3, while 4, 5, 6, and 7 are second neighbors.

H_1 is the base Hamiltonian and $f(x)=x^2+x-(1+2\tau^2)$. The Green functions and DOS are calculated from those of H_1.

To get the LDOS for H_1 at a corner junction, we start iterating Eqs. (87) and (88) *not* from $x=y=1/z$, corresponding to a single site, but rather from the Green function of a seed H corresponding to a triangle with elements τ between the sites. Thus we start from

$$x=(z-\tau)(z+\tau)^{-1}(z-2\tau)^{-1} , \tag{95}$$

$$y=\tau(z+\tau)^{-1}(z-2\tau)^{-1} . \tag{96}$$

Green functions X and Y are found by iteration. To make H_1 uniformly threefold, it is a very good approximation for a large lattice, i.e., after many iterations, simply to connect site l to a site l' of another copy of the lattice. LDOS at the junction site is obtained, using Eq. (81), from

$$D^{(1)}(E)=-\mathrm{Im}[X(1-X^2)^{-1}]/\pi . \tag{97}$$

The LDOS is extended by Eq. (11).

$$D_l(E)=\frac{\Theta(5+8\tau^2+4E)}{[5+8\tau^2+4E]^{1/2}}[D^{(1)}(x_+(E))+D^{(1)}(x_-(E))] , \tag{98}$$

with

$$x_\pm(E)=\tfrac{1}{2}[-1\pm(5+8\tau^2+4E)^{1/2}] . \tag{99}$$

Results for $D_l(E)$, the LDOS at the corner junction of the Sierpiński lattice with Hamiltonian $H+\tau H_2$, are presented in Fig. 8.

Though the inclusion of second neighbors produces substantial changes in the features of the LDOS, scaling exponents such as c and p are not changed. They are determined by what happens at large length scales and thus are not affected by local changes in H. It is also quite clear from the form of Eq. (11) that such modifications cannot induce a continuum in the spectrum, since none of the contributing terms contains a

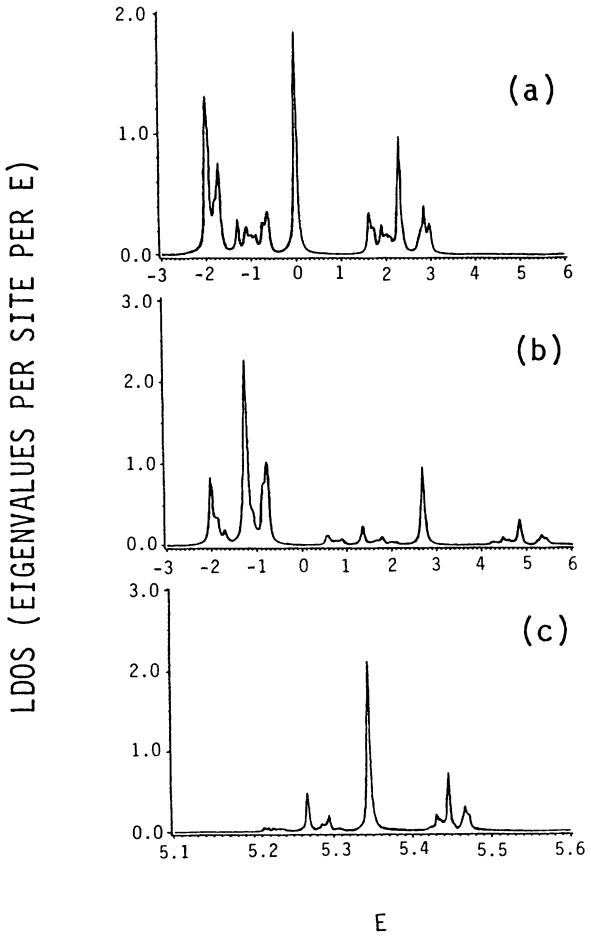

FIG. 8. LDOS at corner junction site l for uniformly threefold Sierpiński Hamiltonians. Each graph represents 20 iterations. (a) First neighbor interactions only. (b) First and second neighbors $H+\tau H_2$. (c) Enlargement of case (b) at higher resolution near E_0. A similar feature is found in case (a) near $E_0=3$.

continuum. We therefore proceed to examine extensions to models on lattices of higher dimension.

The next extension to be considered is

$$H_e=H\otimes I+I\otimes H \tag{100}$$

where H is a threefold Sierpiński Hamiltonian with first-neighbor matrix elements $+1$.

H_e represents a higher dimensional fractal. The sketch in Fig. 9 shows the graphs representing H and H_e when the generation of H is $n=2$. The graph of H_e is variously known as the Cartesian product,[20] or the sum[10] of two of the graphs of H.

The lattice of H_e has linear size $L_e\sim 2^n$ and the number of sites is $N_e=3^{2n}$. Thus the fractal dimension is $\bar{d}_e=2\bar{d}$. In general, the fractal dimensions add. Since $\bar{d}_e=2\ln 3/\ln 2=3.1699\ldots$, the graph of H_e becomes difficult to represent, even in 3D. Each site in the interior or at a facet is sixfold coordinated, as in a cubic lattice. Sites at an edge or corner are five or fourfold coordinated.

The graph of H_e is hierarchical, or self similar, in that

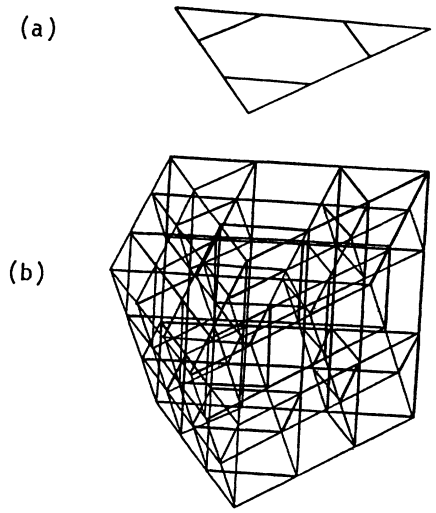

FIG. 9. Sketch of product lattice. (a) Sierpiński Hamiltonian H for generation $n=2$. (b) Corresponding graph for $H\otimes I+I\otimes H$. Note facets consisting of square sublattices.

the graph for generation $n+1$ consists of 9 copies of the graph for generation n, sewn together at the edges by $\mathcal{O}(2^n)$ bonds. It is thus more connected than other hierarchical lattices such as the Sierpiński lattice based on tetrahedra.[12] The latter are connected at only a constant (small) number of sites when generation $n+1$ is formed from generation n.

Figure 10 presents the LDOS for a corner site of the fractal lattice Hamiltonian H_e, as computed by auto convolution of the LDOS of Fig. 5(a). The spectrum extends from -4 to $+6$. The curves show again a rather clear self similarity. We will show that the exponents corresponding to c and p for the new Hamiltonian are $2c+1$ and $2p+1$, and thus that the spectral dimension is $2\bar{\bar{d}}=4\ln 3/\ln 5=2.730\ldots$.

To see how scaling is passed through the extension process, let us suppose $D^{(H)}(E)$ and $D^{(K)}(E)$ each admit a transformation of the form

$$D(E_0-\alpha\,\Delta E)=\alpha^c D(E_0-\Delta E) \tag{101}$$

for small enough ΔE. The upper spectral bound E_0 is E_1 for H and E_2 for K and the exponents are c_1 and c_2. The α is assumed the same for each. In view of Eq. (63),

$$\begin{aligned} D^{(e)}&(E_1+E_2-\alpha\,\Delta E)\\ &=\int_0^{\alpha\,\Delta E} D^{(H)}(E_1-\alpha\,\Delta E+y)D^{(K)}(E_2-y)dy\\ &=\int_0^{\Delta E} D^{(H)}[E_1-\alpha(\Delta E-u)]D^{(K)}(E_2-\alpha u)(\alpha du)\\ &=\alpha^{c_1+c_2+1}D^{(e)}(E_1+E_2-\Delta E)\,. \end{aligned} \tag{102}$$

Thus $D^{(e)}(E)$ is also self similar near the upper bound E_1+E_2 of the spectrum of H_e with exponent $c=c_1+c_2+1$. From $c=\frac{1}{2}\bar{\bar{d}}-1$ it follows that, for this kind of extension, the spectral dimensions also add. We have both $\bar{d}=\bar{d}_1+\bar{d}_2$ and $\bar{\bar{d}}=\bar{\bar{d}}_1+\bar{\bar{d}}_2$. Figure 10 is consistent with $p=p_1+p_2+1$, which follows from the same

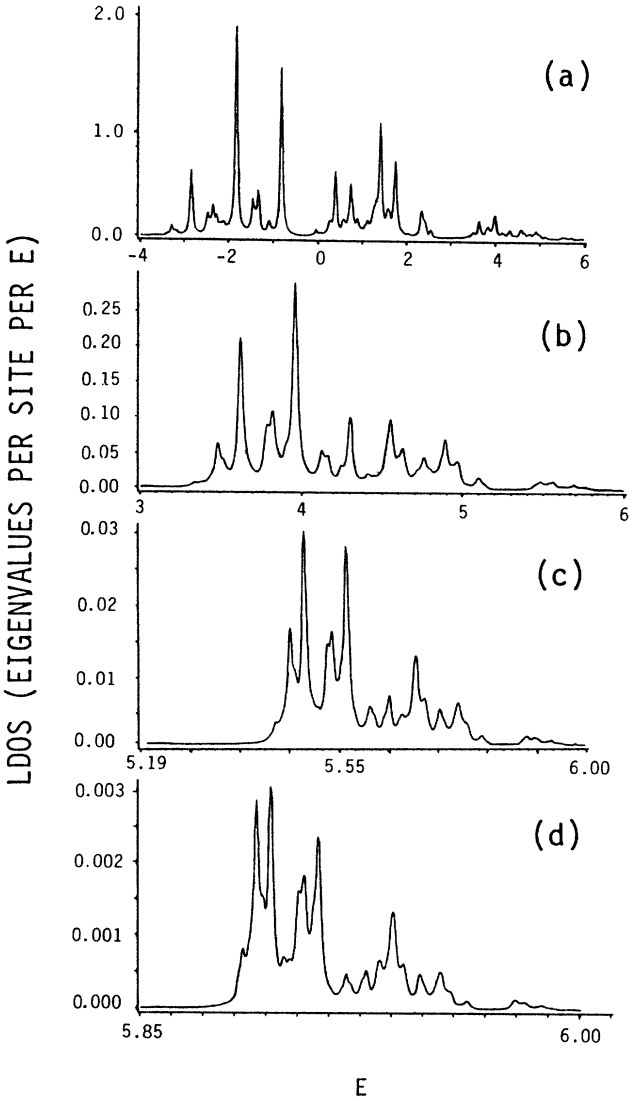

FIG. 10. LDOS for corner site on Cartesian product of two, 20-iteration Sierpiński lattice Hamiltonians. The lattice for the two-iteration case is sketched in Fig. 9. (a) Complete spectrum extending from -4 to $+6$, (b) through (d) successive enlargements at higher resolution near $E_0=+6$ showing self-similarity.

argument applied to the LDOS.

The additivity of both $\bar{d}$ and $\bar{\bar{d}}$, under extensions of the type developed in Eqs. (63) and (64) and the paragraph preceding, implies a sort of conservation of a scaling exponent governing random walks. A long random walk on a fractal lattice can itself be considered a fractal.[26,27] The concept of spectral dimension $\bar{\bar{d}}$ rests on the observation that the fractal dimension[26] of the random walk d_w is given by $d_w=2\bar{d}/\bar{\bar{d}}$, where $\bar{d}$ and $\bar{\bar{d}}$ are the fractal and spectral dimensions of the lattice. Thus, for extensions of this kind, d_w is preserved. In some sense, the fact that $d_w=2$ for nonfractal lattices in any number of Euclidean dimensions[27] is related to the fact that the linear chain, the square lattice, the cubic lattice and so on are related by such an extension. Likewise $d_w=\ln 5/\ln 2$ is preserved for extensions of Sierpiński lattice Hamiltonians.

To conclude this section, it is noted that Rammal and Toulouse[27] have suggested, based on an examination of scaling theory of electrical conductivity[28] that there may be a mobility edge in fractals with $\bar{\bar{d}}$ greater than 2.

V. QUASIPERIODIC LATTICES

The lattice Hamiltonians of this section are based on the 1D Fibonacci Hamiltonian treated by Kohmoto and Banavar.[15] As with the Sierpiński case, we consider not a single Hamiltonian but a family of Hamiltonians corresponding to a sequence of graphs defined as follows. The first graph consists of a single point $(\cdot)$ and the second of two points joined by a bond representing a matrix element of strength b, $(\cdot b\cdot)$. Each succeeding graph is formed by concatenating the previous two and joining them with a bond of strength a. Symbolically, $H_n=(H_{n-1})a(H_{n-2})$. Thus, the graphs corresponding to the first several Hamiltonians are

$$\begin{aligned} &H_1=\cdot\ , \\ &H_2=\cdot b\cdot\ , \\ &H_3=(\cdot b\cdot)a(\cdot)=\cdot b\cdot a\cdot\ , \\ &H_4=(\cdot b\cdot a\cdot)a(\cdot b\cdot)=\cdot b\cdot a\cdot a\cdot b\cdot\ , \\ &H_5=(\cdot b\cdot a\cdot a\cdot b\cdot)a(\cdot b\cdot a\cdot)=\cdot b\cdot a\cdot a\cdot b\cdot a\cdot b\cdot a\cdot\ , \\ &\cdots\ . \end{aligned} \tag{103}$$

If another bond of strength a were appended to the left of each graph the a and b bonds would occur in a Fibonacci sequence. The ratio of b to a bonds approaches the Fibonacci ratio τ as the number of sites goes up.

The 1D Fibonacci lattices are interesting primarily owing to their relationship to the 2D Penrose lattice.[29,30] The Penrose lattice has three significant properties. It is quasiperiodic, admits inflation-deflation transformations, and has a remarkable sort of fivefold rotation symmetry.

In the current section, after solution of the 1D Fibonacci problem by the synthetic method is outlined, the results are extended to a study of 2D and 3D Fibonacci plaids which, like the Penrose lattice, are quasiperiodic and admit inflation-deflation transformations, but, unlike the Penrose case, do not have forbidden rotation symmetry.

Consider the formal recursion $H_n=H_{n-1}aH_{n-2}$, let sites 1 and 2 be at the left and right of the lattice of H_{n-1}, and let 3 and 4 be at the left- and right-hand sides of the lattice of H_{n-2}. Denote by V in Eq. (81) the matrix elements connecting sites 2 and 3 to form H_n. One solves for $x_n=aG_{11}(z)$, $y_n=aG_{44}(z)$, and $z_n=aG_{14}(z)$ in terms of the corresponding $x_{n-1}=ag_{11}(z)$, $y_{n-1}=ag_{22}(z)$, $z_{n-1}=ag_{12}(z)$ and $x_{n-2}=ag_{33}(z)$, $y_{n-2}=ag_{44}(z)$, and $z_{n-2}=ag_{34}(z)$. The resulting recursion formulas are

$$\Delta_n=1-x_{n-1}y_n\ , \tag{104}$$

$$x_{n+1}=x_n+x_{n-1}z_n^2/\Delta_n\ , \tag{105}$$

$$y_{n+1}=y_{n-1}+y_nz_{n-1}^2/\Delta_n\ , \tag{106}$$

$$z_{n+1}=z_{n-1}z_n/\Delta_n\ . \tag{107}$$

These are iterated starting from

$$x_0=y_0=z_0=a/z \ , \tag{108}$$

$$x_1=y_1=az(z+b)^{-1}(z-b)^{-1} \ , \tag{109}$$

$$z_1=ab(z+b)^{-1}(z-b)^{-1} \ . \tag{110}$$

Again, as in the Sierpiński case, one could instead choose another seed Hamiltonian. With $z=E+i\eta$, LDOS for the left and right end sites are obtained from

$$D_1(E)=-\mathrm{Im}[x_{n+1}]/\pi a \ , \tag{111}$$

$$D_4(E)=-\mathrm{Im}[y_{n+1}]/\pi a \ . \tag{112}$$

For the connection sites, one has

$$D_2(E)=-\mathrm{Im}[y_n/\Delta_n]/\pi a \ , \tag{113}$$

$$D_3(E)=-\mathrm{Im}[x_{n-1}/\Delta_n]/\pi a \ . \tag{114}$$

Figure 11 illustrates various properties of the 1D Fibonacci lattice, all of which have been investigated by others.[15,16,31–34]

The LDOS on site 1, the end site of the 25th generation lattice, is shown in Fig. 11(a). There are 1.2×10^5 sites in generation 25. The parameter values are $a=0.9$ and $b=1$. If both a and b were 1, as in an ordered chain, a smooth elliptical LDOS extending from $E=-2$ to $E=2$ would result. Figures 11(b) and 11(c) show the central portion at successively higher resolution, demonstrating self similarity of the LDOS near $E=0$. This has been noted by several authors,[32] and can be related to the inflation-deflation symmetry.[15]

Inflation-deflation symmetry[14,15] of the sequence of graphs introduced above operates as follows. If the two end sites of each graph in the sequence are connected by an a bond, thus forming the graphs into rings, then the replacement $a\rightarrow a\cdot b$ and $b\rightarrow a$ takes the nth graph into the $(n+1)$th, thus defining the inflation symmetry. Deflation goes the other way.

Since on a very large graph, a bond subsequence of length L always repeats itself within a length proportional to L, the spectral features near the ground state $E=E_0$, corresponding to long wavelengths, become similar to those of a uniform lattice. Figure 11(d) shows the E range near E_0 for the LDOS at the interior site 2 for the 25th generation lattice with $a=0.99$ and $b=1$. The structure of the 1D Van Hove singularity is apparent in

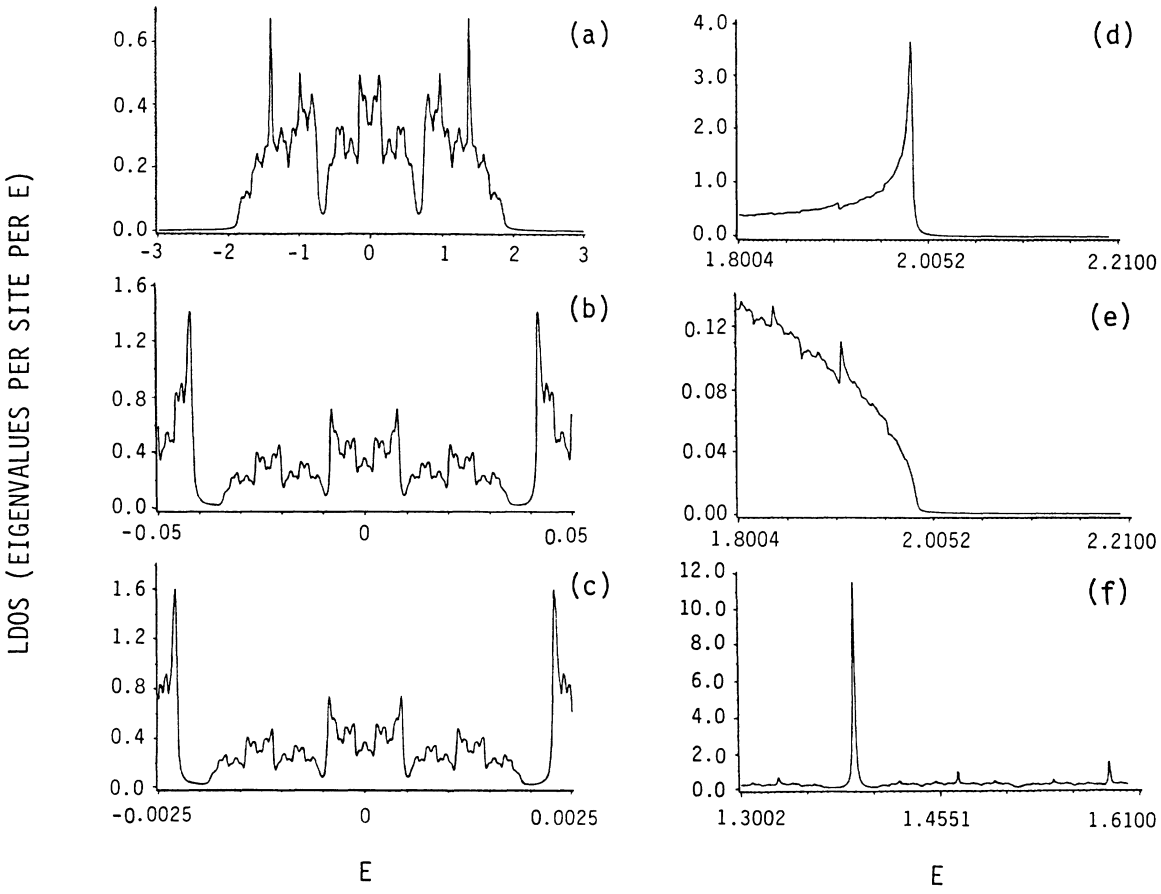

FIG. 11. LDOS for sites of 1D Fibonacci lattice Hamiltonian, 25 iterations. (a) Complete spectrum for end site 1, $a=0.9$, $b=1$. (b) Enlargement at higher resolution near $E=0$. (c) Enlargement at higher resolution showing self-similarity. (d) E near E_0 at inner site 2 showing a Van Hove singularity. In this case, $a=0.99$, $b=1$. (e) End site 1 for same lattice showing how the LDOS approaches the singular behavior of an ordered lattice close to the ground state at E_0. (f) Surface state peaks, $a=0.9$, $b=1$.

the figure. Figure 11(e) shows the LDOS for the end site 1 for the same lattice Hamiltonian. The limiting curve at E close to E_0 is approaching the smooth ellipse of a uniform lattice, again with a perfect Van Hove singularity.[15,32]

The isolated peaks in Fig. 11(f) correspond to *bona fide* surface states with wave functions localized near the ends of the chain. Reduction of η for a fixed energy range causes these isolated peaks to grow relative to other spectral features. Surfaces states are discussed by Liu and Riklund[34] for chains with diagonal Fibonacci disorder.

Results for the 1D Fibonacci lattice Hamiltonians are extended to higher dimensions by the methods of Sec. III. Figure 12 illustrates a 2D Fibonacci plaid formed from two copies of the lattice of the generation 5 Fibonacci Hamiltonian in 1D. In general, the Hamiltonian of a 2D Fibonacci plaid H_e is defined by

$$H_e = H \otimes I + I \otimes H \tag{115}$$

where H is a 1D Fibonacci lattice Hamiltonian. Fibonacci plaids in 3D are similarly defined.

The 2D and 3D Fibonacci plaids inherit inflation-deflation properties from the 1D components. For example, in Fig. 12 there are three kinds of square cells. Those with no dark line inflate into a single square with all dark lines. Those with two parallel dark lines inflate into a rectangle consisting of a square with all dark sides and one with two dark sides. The squares with all dark sides go into a large square composed of one square with all dark lines, two with two dark lines, and one with none. The dark lines represent a bonds and the dashed ones b bonds.

Figure 13 shows LDOS for interior sites on 2D and 3D plaids. These are obtained via Eq. (63) by numerical convolutions involving the 1D results. Figure 13(a) is the LDOS for a site interior to a 2D plaid found by autoconvolution of $D_2(E)$ from Eq. (113). The linkage strengths are $a=0.9$ and $b=1$. Increasing the resolution does *not* uncover significantly more complex structure. Two-dimensional dispersion has broadened the self-similar features and isolated peaks into a relatively smooth continuum. The general shape is like that of the square-lattice result shown in Fig. 1(a). Choy[35] has presented numerical results for the LDOS of a typical threefold coordinated site on the Penrose lattice and speculated that there is a well-defined Van Hove singularity at $E=0$ in the Penrose case. However, Kohmoto and Sutherland showed that what had appeared to be a sharp Van Hove singularity in the Penrose LDOS actually represents a gap containing a localized state at $E=0$.[36] In contrast, the LDOS shown for the 2D plaid *does* have a rather sharp Van Hove singularity resulting via convolution form the well-formed bandedge singularities as shown in Fig. 11(d).

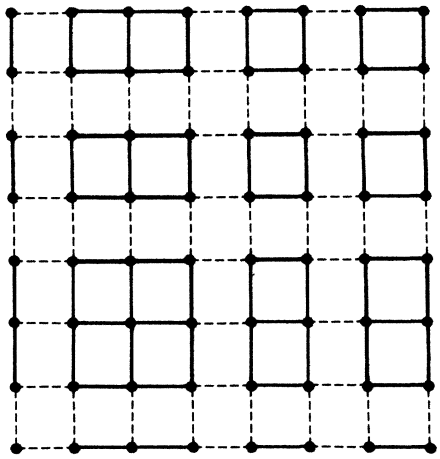

FIG. 12. Graph corresponding to 2D Fibonacci plaid. Solid lines represent a bonds and dashed lines b bonds. The Hamiltonian is $H_e = H \otimes I + I \otimes H$, where H is the five-iteration 1D Fibonacci Hamiltonian.

Figures 13(b) through 13(d) show LDOS at interior sites of a 3D Fibonacci plaid. In each case, $b=1$. The parameter a is 0.99 in Fig. 13(b), 0.90 in Fig. 13(c), and 0.50 in Fig. 13(d). The similarity between Fig. 13(a) and Fig. 2(a) is evident. The smooth, bell-shaped curve of Fig. 13(c) shows no trace of the structure present in 1D for the same parameter values. In the limit of $a \to 0$, the LDOS reduces to a few isolated peaks as the lattice decomposes into disconnected molecules.

Since eigenvectors of the plaid Hamiltonians consist of direct products of eigenvectors of the 1D Fibonacci case, as in Eq. (43), the eigenstates are localized or delocalized to the same degree. The extent of localization in a 1D Fibonacci model is discussed by several authors.[16,31]

A measure of eigenstate localization in the one-electron problem is the electrical conductivity. The expression

$$\sigma(E) = \frac{\pi}{N} \mathrm{Tr}[\tilde{G}(E+i\eta) p \tilde{G}(E+i\eta) p] \tag{116}$$

for conductivity[37,38] is extended by the preceding techniques from the 1D chain result to the plaid lattices. In Eq. (116), N is the number of sites, p is a component of the momentum operator, and for simplicity, the notation

$$\tilde{G}(E+i\eta) = -\frac{1}{\pi} \mathrm{Im}[G(E+i\eta)] \tag{117}$$

is used. A convenient technique for computing Eq. (116) for chains has recently been reported by Thouless and Kirkpatrick.[38] To obtain an extension formula, consider the Hamiltonian $H_e = H \otimes I + I \otimes K$. Suppose the momentum component p is taken perpendicular to the sublattice of K, so that

$$p_{(kl)(mn)} = p^{(H)}_{km} \delta_{ln} , \tag{118}$$

then on substituting Eq. (64) for $\tilde{G}(E+i\eta)$ into Eq. (116), one finds

$$\sigma_e(E) = \int_{-\infty}^{\infty} \int_{-\infty}^{\infty} T^{(H)}(x,y) Q^{(K)}(E-x, E-y)\, dx\, dy \tag{119}$$

where

$$T^{(H)}(x,y) = \sum_{i,k,m,p} [\tilde{G}^{(H)}_{ik}(x+i\eta) p^{(H)}_{km} \tilde{G}^{(H)}_{mp}(y+i\eta) p^{(H)}_{pi}] , \tag{120}$$

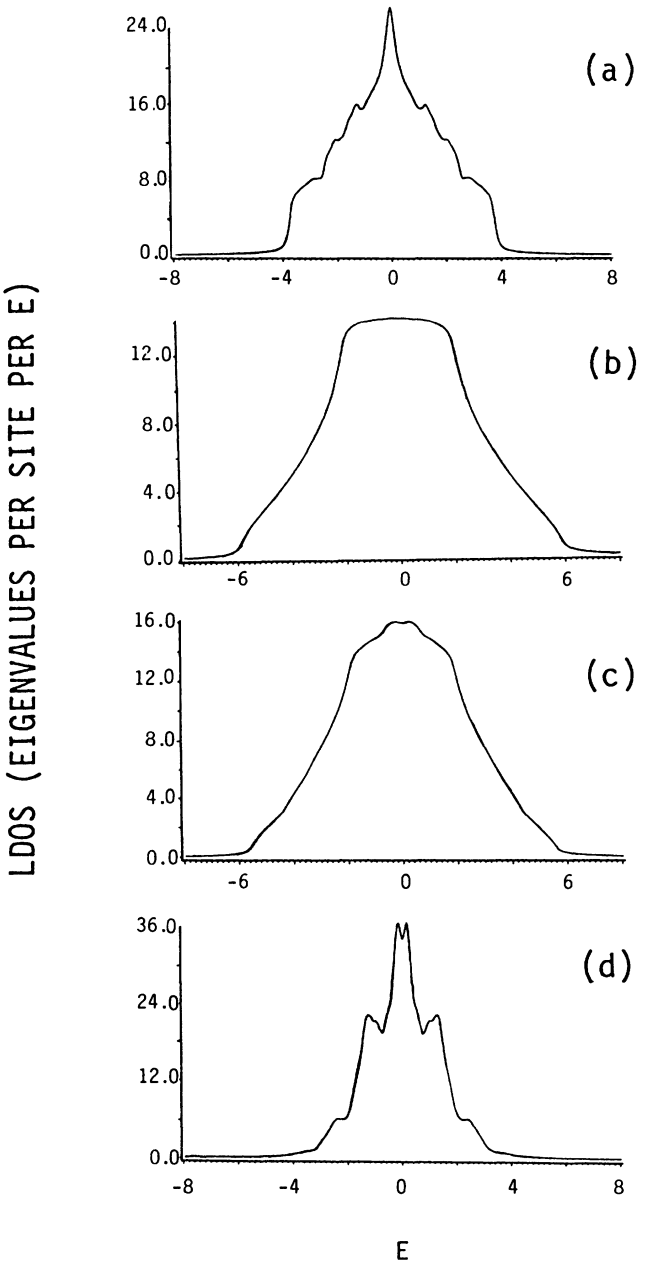

FIG. 13. LDOS for interior sites of 2D and 3D Fibonacci plaids. (a) 2D plaid with $a=0.9$, $b=1$. (b) through (d) 3D plaids with $b=1$, and with $a=0.99$, 0.9, and 0.5, respectively.

and

$$Q^{(K)}(E-x,E-y) = \sum_{l,j} \tilde{G}^{(K)}_{jl}(E-x+i\eta)\tilde{G}^{(K)}_{lj}(E-y+i\eta) . \quad (121)$$

But, in view of Eq. (50), $Q^{(K)}(E-x,E-y)$ reduces to

$$Q^{(K)}(E-x,E-y)=\delta(x-y)D^{(K)}(E-x) . \quad (122)$$

Whence the conductivity is simply

$$\sigma_e(E)=\int_{-\infty}^{\infty}\sigma^{(H)}(x)D^{(K)}(E-x)dx \quad (123)$$

with $\sigma^{(H)}(E)$ the conductivity corresponding to H, and $D^{(K)}(E)$ the DOS per site for K. Thus the relationship between the conductivities of the plaid lattices and the conductivity of the 1D chain is trivial.

VI. CONCLUSION

The major intent of the preceding sections is to establish a formalism for using Green functions corresponding to Hamiltonian H to obtain Green functions for a related Hamiltonian $H_e=f(H)$, where f is a rational function. The essential result is Eq. (16) which expresses the Green functions $G^{(e)}(z)$ for H_e in terms of those $G(z)$ for H. A convenient formula is given in Eq. (11) extending the DOS and LDOS of H to those of H_e without reference to the Green functions. Thus DOS or LDOS obtained by any means, including the digitizing of published curves, can be extended to results for other Hamiltonians. The constraint that H_e must be of the form $f(H)$ in order to make use of the extension procedure for an H with known solutions is quite severe. Nevertheless, as the examples of Sec. II show, the extension formulas give results that are useful both formally and numerically for physically interesting models.

The formalism is further developed in Sec. III to permit extending the Green functions of two lattice Hamiltonians H and K, defined on the same or different lattices, to any Hamiltonian H_e in the algebra generated by the direct product matrices $H\otimes I$ and $I\otimes K$, as defined in Eq. (3). The major result is Eq. (52) expressing $G^{(e)}(z)$ in terms of $G^{(H)}(z)$ corresponding to H, and $G^{(K)}(z)$ corresponding to K. The linear homogeneous case, being of particular interest, is given in simplified form in Eq. (64). Separate formulas for the DOS and LDOS are presented in Eqs. (46) and Eq. (63). The formal efficiency of these equations is illustrated in Sec. III, where expressions for Green functions and LDOS for several models are developed; in Sec. III, where scaling exponents are examined, and in Sec. V, where electrical conductivity $\sigma(E)$ is extended from 1D to 2D and 3D models. The numerical usefulness of the extension formulas is illustrated throughout Secs. IV and V by their application to the exploration of several fractal lattices and quasiperiodic lattices.

The fact that these extension techniques give an efficient way of computing lattice Green functions for regular lattice models is of practical interest. It is appropriate to ask, however, whether the new models made accessible by these methods, such as the fractal and quasiperiodic models described above, are genuinely interesting. For example, do they contain any nontrivial physics not already contained in the base Hamiltonians H and K? This question is suggested particularly by the remarks at the end of Sec. V concerning localization and conductivity in the one-electron problem.

It is generally expected that $\sigma(E)$ for a disordered lattice of dimension 2 or less should tend to zero for each E as the size of the lattice increases, for any degree of disorder. For higher dimensions, some states may be localized and others not, so that $\sigma(E)$ may not tend to zero for a certain set of E values.[28] The situation seems more com-

plicated for quasiperiodic order.[15,16,31,32] Anderson[39] originally associated the localization of eigenstates with a noncontinuum structure of the spectrum. Where the spectrum is not a continuum, states are localized. But, when the spectrum does contain a continuum, to what extent must the eigenstates be delocalized?

As mentioned in Sec. V, eigenstates of the model $H_e = H \otimes I + I \otimes H$ are localized to the same degree as those of H.[41] It is interesting to note, however, that even though there may be no continuum in the spectrum of H, or K, the eigenvalues may condense under convolution so that the spectrum of H_e *can* contain a continuum. We offer the following argument.

Let H represent the fourfold Sierpiński Hamiltonian, the spectrum of which contains no continuum. That is, there is no continuous range of eigenvalues without a gap. A subset of eigenvalues of H resembles the Cantor set in that it consists of the set that remains when an infinite sequence of nested gaps is created in a closed interval.[12,27] This situation is typical of the spectra of hierarchical lattices and also appears to occur for the 1D Fibonacci case.[31,32]

The Cantor set[40] is a nowhere dense, perfect subset of the closed interval [0,1]. It is the subset remaining after an infinite deletion process in which, at each stage, the open middle $\frac{1}{3}$ is removed from each remaining subinterval. Its elements consists of all numbers E with the ternary representation

$$E = \sum_{n=1}^{\infty} a_n 3^{-n} , \tag{124}$$

with each a_n an element of the two-element set $\{0,2\}$.

The spectrum of H_e consists of the set of sums of all pairs of elements of the spectrum of H, i.e., it is the auto convolution of the spectrum of H. Since the spectrum of H contains a Cantor-like subset, we form the auto convolution of the Cantor set. This must contain all numbers E' of the form

$$E' = \sum_{n=1}^{\infty} b_n 3^{-n} , \tag{125}$$

with b_n an element of $\{0,2,4\}$. But this is the ternary representation of an arbitrary number in [0,2]. Thus the convolution contains the whole interval.

If one modifies the constructive definition of the Cantor set so that, rather than removing the open middle $\frac{1}{3}$ from each subinterval at each step, the gap ratio $r = \frac{1}{3}$ is replaced by $r = (k-2)/k$ for integer k, the resulting set contains of all numbers with k-ary representation

$$E = \sum_{n=1}^{\infty} a_n k^{-n} , \tag{126}$$

with each a_n in the set $\{1, k-1\}$. The $k-2$ fold convolution will contain the interval $[0, k-1]$, but no fewer convolutions will produce condensation.

The foregoing analysis suggests the existence of a condensation transition from noncontinuum to continuum spectral character as a function of a gap ratio r characteristic of the base Hamiltonian H.[41] A criterion for condensation after $k-2$ convolutions would $b(k-2)/k > r$. For the fourfold coordinated Sierpiński Hamiltonian, Domany *et al.*[12] report $r = 0.424\,643\ldots$ or $r = (\beta - 1)/\beta$ in their notation. Thus, for condensation, $k - 2 = 1.476\,15\ldots$ or two convolutions would be required.

Gap ratios for the 1D Fibonacci spectrum vary as a function of the coupling constants.[32] Starting with an H of this sort in 1D, one can make 2D and 3D plaid models to look for a spectral condensation as a function of r. Since gap ratios may differ in different parts of the spectrum of H, there may be cases in which the spectrum of H_e contains a continuum for some range of energy but is noncontinuous elsewhere. This is somewhat analogous to the existence of a mobility edge which would separate a range of eigenvalues corresponding to localized states from a range corresponding to extended states.[27,28] It is unclear to what extent the transition from continuum to noncontinuum spectral properties relates to a transition from extended to localized eigenstates on disordered lattices.

We therefore conclude that the extension formalism reported here enables the treatment of a variety of lattice Hamiltonians which, besides being of practical use in exploring dynamical phenomena on regular lattices and superlattices, may be theoretically interesting in their own right.

ACKNOWLEDGMENTS

The authors thank Michael Gregory for a useful discussion concerning perfect sets, and for bringing Ref. 41 to our attention. One of us (W.S.) is also pleased to have attended a series of lectures by Allen Shwenk as part of the Summer Seminar on Graph Theory and Linear Algebra (Duluth, 1987) of the Mathematical Association of America.

[1]F. Dyson, Phys. Rev. **92**, 1331 (1953).
[2]S. Davison and J. Levine, Solid State Phys. **25**, 1 (1970).
[3]R. Bass, J. Math. Phys. **26**, 3068 (1985).
[4]S. Katsura, T. Morita, S. Inawashiro, T. Horiguchi, and Y. Abe, J. Math. Phys. **12**, 892 (1971), and references therein.
[5]T. Morita and T. Horiguchi, J. Phys. Soc. Jpn. **30**, 957 (1971); J. Math. Phys. **12**, 981 (1971).
[6]T. Morita and T. Horiguchi, J. Math. Phys. **12**, 986 (1971).
[7]T. Morita, J. Math. Phys. **12**, 1744 (1971).
[8]T. Morita and T. Horiguchi, J. Math. Phys. **13**, 1243 (1972).
[9]T. Horiguchi, J. Math. Phys. **13**, 1411 (1972).
[10]D. Cvetković, M. Doob, and H. Sachs, *Spectra of Graphs and Applications* (Academic, New York, 1980), pp. 65–72; and references therein.
[11]Y. Gefen, A. Ahrony, B. Mandelbrot, and S. Kirkpatrick, Phys. Rev. Lett. **47**, 1771 (1981).
[12]E. Domany, S. Alexander, D. Bensimon, and L. Kadanoff, Phys. Rev. B **28**, 3110 (1983).

[13]S. Alexander, Phys. Rev. B **29**, 5504 (1984).
[14]P. Steinhart, Am. Sci. **74**, 586 (1986).
[15]M. Kohmoto and J. Banavar, Phys. Rev. B **34**, 563 (1986).
[16]J. Verges, L. Brey, E. Louis, and C. Tejedor, Phys. Rev. B **35**, 5270 (1987).
[17]J. Friedel, Adv. Phys. **3**, 446 (1954).
[18]R. Haydock, V. Heine, and M. J. Kelly, J. Phys. C **5**, 2845 (1972).
[19]W. Schwalm and M. Schwalm, Am. J. Phys. **51**, 230 (1983).
[20]A. Shwenk and R. Wilson, in *Selected Topics in Graph Theory,* edited by L. Beineke and R. Wilson (Academic, London, 1978).
[21]K. Knopp, *Theory of Functions* (Dover, New York, 1947), Vol. 2.
[22]C. Zaspel (unpublished).
[23]E. Whittaker and G. Watson, *Course in Modern Analysis* (Cambridge University Press, Cambridge, 1958), p. 507.
[24]S. Freeman, Phys. Rev. B **2**, 3272 (1970).
[25]B. O'Shaughnessy and I. Procaccia, Phys. Rev. A **32**, 3073 (1985).
[26]S. Alexander and R. Orbach, J. Phys. Lett. (Paris) **43**, L625 (1982).
[27]R. Rammal and G. Toulouse, J. Phys. Lett. (Paris) **44**, L13 (1983).
[28]E. Abrahams, P. Anderson, D. Licciardello, and D. Ramakrishnan, Phys. Rev. Lett. **42**, 673 (1979).
[29]R. Penrose, Bull. Inst. Math. Appl. **10**, 266 (1974).
[30]M.Gardner, Sci. Am. **236**, 110 (1977).
[31]M. Kohmoto, L. Kadanoff, and C. Tang, Phys. Rev. Lett. **50**, 1870 (1983).
[32]J. Lu, T. Odagaki, and J. Birman, Phys. Rev. B **33**, 4809 (1968).
[33]F. Nori and J. Rodrigues, Phys. Rev. B **34**, 2207 (1968).
[34]Y. Liu and R. Riklund, Phys. Rev. B **35**, 6034 (1987).
[35]T. Choy, Phys. Rev. Lett. **55**, 2915 (1985).
[36]M. Kohmoto and B. Sutherland, Phys. Rev. Lett. **56**, 2740 (1986); and Phys. Rev. B **34**, 3849 (1986).
[37]G. Czycholl and B. Kramer, Solid State Commun. **32**, 945 (1979).
[38]D. Touless and S. Kirkpatrick, J. Phys. C **14**, 235 (1981).
[39]P. Anderson, Phys. Rev. **109**, 1492 (1958).
[40]R. Boas, *A Primer of Real Functions* (Wiley, New York, 1960).
[41]J. Skinner, MSc. thesis, University of North Dakota, 1973.